

The Composition of Centaur 5145 Pholus

D. P. Cruikshank¹

NASA Ames Research Center, MS 245–6, Moffett Field, California 94035-1000
E-mail: cruikshank@ssa1.arc.nasa.gov

T. L. Roush

NASA Ames Research Center, MS 245-3, Moffett Field, California 94035-1000

M. J. Bartholomew

Sterling Software and NASA Ames Research Center, MS 245-3, Moffett Field, California 94035-1000

T. R. Geballe

Joint Astronomy Centre, 660 North A'ohoku Place, University Park, Hilo, Hawaii 96720

Y. J. Pendleton

NASA Ames Research Center, MS 245–3, Moffett Field, California 94035-1000

S. M. White

NASA Ames Research Center, MS 234-1, Moffett Field, California 94035-1000

J. F. Bell, III

CRSR, Cornell University, Ithaca, New York 14853

J. K. Davies

Joint Astronomy Centre, 660 N. A'ohoku Place, University Park, Hilo, Hawaii 96720

T. C. Owen¹

Institute for Astronomy, 2680 Woodlawn Drive, Honolulu, Hawaii 96822

C. de Bergh¹

Observatoire de Paris, 5 Place Jules Janssen, 92195 Meudon Cedex, France

D. J. Tholen¹

Institute for Astronomy, 2680 Woodlawn Dr., Honolulu, Hawaii 96822

M. P. Bernstein

SETI Institute and NASA Ames Research Center, MS 245–6, Moffett Field, California 94035-1000

R. H. Brown

Lunar and Planetary Laboratory, Univ. of Arizona, Tucson, Arizona 85721

¹ Guest observer at the United Kingdom Infrared Telescope (UKIRT). UKIRT is operated by the Joint Astronomy Centre on behalf of the United Kingdom Particle Physics and Astronomical Research Council.

K. A. Tryka

Dept. of Physics, Northern Arizona University, Flagstaff, Arizona 86011

and

C. M. Dalle Ore

SETI Institute and NASA Ames Research Center, MS 245-6, Moffett Field, California 94035-1000

Received April 29, 1996; revised June 29, 1998

We present a new spectrum of the Centaur object 5145 Pholus between 1.15 and 2.4 μm . We model this, and the previously published (0.4- to 1.0- μm) spectrum, using Hapke scattering theory. Seen in absorption are the 2.04- μm band of H_2O ice and a strong band at 2.27 μm , interpreted as frozen methanol and/or a photolytic product of methanol having small molecular weight. The presence of small molecules is indicative of a chemically primitive surface, since heating and other processes remove the light hydrocarbons in favor of macromolecular carbon of the kind found in carbonaceous meteorites. The unusually red slope of Pholus' spectrum is matched by fine grains of a refractory organic solid (tholin), as found previously by M. Hoffmann *et al.* (1993, *J. Geophys. Res.* 98, 7403–7407) and P. D. Wilson *et al.* (1994, *Icarus* 107, 288–303). Olivine (which we model with Fo 82) also appears to be present on Pholus. We present a five-component model for the composite spectrum of all spectroscopic and photometric data available for 5145 Pholus and conclude that this is a primitive object which has not yet been substantially processed by solar heat. The properties of Pholus are those of the nucleus of a large comet that has never been active. © 1998 Academic Press

Key Words: asteroids, composition; comets, composition; ices, centaurs; prebiotic chemistry.

1. INTRODUCTION

1.1. Discovery

On 9 January 1992, the Spacewatch asteroid search project discovered object 1992 AD, now designated 5145 Pholus, in a highly eccentric orbit that passes from a perihelion point just inside the orbit of Saturn to well outside the orbit of Neptune at aphelion, with a period of 92.7 years (Scotti 1992, Marsden 1992). Pholus is one of the family of bodies known as Centaurs, that is, objects with orbits crossing those of the outer planets. Measurements of the thermal flux (Howell *et al.* 1992) indicate that the diameter of Pholus is at least 140 km and the albedo is <0.08 at 0.55 μm . Similar thermal flux measurements (Davies *et al.* 1993a) suggest a minimum diameter of about 190 km and albedo (at 0.55 μm) of 0.04. Photometric observations (Buie and Bus 1992, Hoffmann *et al.* 1993) yield a rotation period of 9.98–9.99 h (corroborated by Davies *et al.* 1998) and suggest that the object is irregular in shape.

The short dynamical lifetime of Pholus in its present orbit (e.g., Levison and Duncan 1993), plus its red color and spectral properties, strongly suggest that it recently entered the planetary zone from the Kuiper Disk of planetesimals. Because the Kuiper Disk is the source of the low-inclination comets, and because of the compositional similarities of Pholus to comets, it is reasonable to conclude that Pholus is a primitive body that has not experienced large-scale sublimation or chemical processing through heating by the Sun. Instead, it has spent all but the past 10^6 to 10^7 years of its existence in the frozen state beyond about 30 AU from the Sun.

While the orbit of Pholus is comet-like, its dimensions are an order of magnitude greater than those of a typical comet nucleus and are more similar to many asteroids. Pholus does not clearly fall into either classification. Indeed, both classifications have become rather indistinct in recent years, with the realization from orbital dynamics that some objects long considered asteroids are inactive comets (e.g., Hartmann *et al.* 1986) and the detection of cometary activity in some objects designated as asteroids (Meech and Belton 1990). Further, recent discoveries of numerous small bodies beyond the orbit of Neptune (Jewitt and Luu 1995) challenge the traditional definitions of both comets and asteroids.

At the time of this writing, no spectroscopic or direct imaging evidence for cometary activity has been detected on Pholus.

1.2. Photometric and Spectrophotometric Observations

Photometric and spectrophotometric observations made shortly after the discovery showed that Pholus was the reddest object in the Solar System measured to that time (Mueller *et al.* 1992, Fink *et al.* 1992, and Binzel 1992). In this context, “red” means that, with the color of the Sun removed, the spectral reflectance of the body increases toward longer wavelengths over the interval 0.3–1 μm . Each of the observing groups referenced above independently proposed that the surface of the object is covered, at least in part, by organic solids which impart the extraordinary red color, and low reflectance at wavelength 0.55 μm . Refractory organic solids produced in experiments in which energy is deposited in gases and in ices

exhibit a red color similar to that of Pholus (e.g., Thompson *et al.* 1987, 1991, Strazzulla and Johnson 1991). However, it is difficult to establish an identification of a specific substance on the basis of the reddening characteristic alone.

Organic solids were found in the dust of Comet Halley by experiments on three spacecraft (e.g., Kissel and Krueger 1987); the dust particles contain about 15–35% organic solid, while the remaining inorganic fraction is primarily Mg-rich silicates (pyroxene and/or olivine) (Schulze *et al.* 1997, Fomenkova 1997). Greenberg (1982) and others predicted the refractory organic component of comet dust from studies of interstellar dust.

Apart from methane, specific organic molecules in the solid state have not been identified by remote sensing observations of the surfaces of other Solar System objects, primarily because it is possible to observe only a small portion of the infrared spectrum where diagnostic absorptions occur. The situation is further complicated by the vast number of possible molecular combinations of even a small number of carbon and hydrogen atoms. One can, however, search for evidence of functional groups, such as methyl (CH_3) and methylene (CH_2), as revealed by the frequencies of the stretching and deformations of their chemical bonds. Unfortunately, the fundamentals of these bonds occur in the infrared at $\lambda > 3 \mu\text{m}$, while our observational window for faint Solar System bodies is currently constrained (by technology) to $\lambda \leq 2.5 \mu\text{m}$. We must therefore search for molecular identifications through relatively weak overtone bands (of the fundamental frequencies) as well as combinations of stretching, bending, and scissoring frequencies of the various chemical bonds that hold a given molecule together. Within the framework of this poorly constrained problem, ambiguous and nonunique identifications are to be expected.

1.3. Spectroscopic Observations

An infrared spectrum (1.4–2.4 μm) of 5145 Pholus obtained by Davies *et al.* (1993b) in 1992 showed a strong absorption band centered near 2.27 μm , absorption at 2.0 μm , and other less distinct structure at shorter wavelengths. Davies *et al.* (1993b) noted a resemblance to an absorption band in the tholins described by Sagan and Khare (1979; reflectance spectra are shown in Cruikshank *et al.* (1991)); however, a firm identification of this organic solid could not be made. Wilson *et al.* (1994) explored the comparison with tholins more thoroughly and on the basis of calculated reflectance spectra proposed mixtures of a specific tholin, HCN polymer, and H_2O and NH_3 ices. We return to this work below. Cruikshank *et al.* (1993) noted the similarity in the position and shape of the 2.27- μm Pholus band to that in terrestrial organic solids which are rich in light soluble hydrocarbons (bitumen). The authors proposed that Pholus' surface contains small (light) hydro-

carbon molecules indicating a more chemically primitive surface than exhibited by the D- and C-type asteroids and comets. Luu *et al.* (1994) also observed the 2.27- μm Pholus band; however, they pointed out the dissimilarity to the bitumen band in terrestrial tar sand. At this time, we do not see evidence of a match between bitumen and the Pholus 2.27- μm band, although the final identification of the band will likely be a substance which is rich in light soluble hydrocarbon.

Two of the three observational data sets for the photo-visual spectral region (Fink *et al.* 1992, Binzel 1992) are in good agreement with each other, with relatively minor differences in the steep red slope. The spectral reflectance derived by Mueller *et al.* (1992), however, is less steeply sloped toward the red. While some of these differences may result from the different solar phase angles at the time of the observations (Wilson *et al.* 1994), systematic errors in the flux calibration, induced by the standard stars used, may also contribute. For present purposes we regard the spectral region 0.3–1.0 μm sufficiently well determined and do not offer any new observations. We adopt the redder slopes of the data by Fink *et al.* (1992) and Binzel *et al.* (1992).

In this paper we describe the detailed modeling of the 0.4- to 2.5- μm spectrum of Pholus using the Hapke scattering theory and astrophysically and chemically plausible materials. The origin of these components in the interstellar medium and the effect of various processing mechanisms (UV photolysis, ion bombardment, and heat) are discussed.

2. ANALYSIS OF THE INFRARED SPECTRUM

2.2. New Spectral Data

Our first task has been to obtain improved spectral data for Pholus in the near-infrared (1.2–2.5 μm) in order to provide the basis for a more specific identification of solids on the surface. Because Pholus is very faint, we have been able to obtain only parts of the spectrum during several observing sessions. In this paper we present a composite spectrum derived from our own observations and those of Luu *et al.* (1994).

The improved spectral data (1.15–2.4 μm) reported here were obtained on several occasions in 1992–1995, with the United Kingdom Infrared Telescope and the Cooled Grating Spectrometer-4 (CGS4) (Table I). CGS4 is a cryogenic spectrometer using a diffraction grating and a two-dimensional InSb array detector. We normally used the system in the low-resolution mode (first order of the 75 lines/mm grating, 150 mm focal length camera), which at 1.6 μm gave resolution $R = \lambda/\Delta\lambda = 250$, and at 2.2 μm $R = 340$. Until early 1995, CGS4 used a 58×62 -pixel detector array; with the grating and camera configuration noted, a single setting of the grating gave a spectral interval

TABLE I
Spectra of Pholus

Date (UT)	R (AU)	Delta (AU)	i (deg)	Region covered (μm)	Quality (Weight) ^a	Primary standard
1992 Mar. 26.3	8.724	8.323	6.14	1.45–2.43	Good (2)	BS2890
1993 Jan. 20.5 ^b	8.932	7.994	2.03	1.43–2.45	— (3)	—
1993 Feb. 4.4	8.959	7.982	0.94	2.04–2.46	Excellent (4)	BS4030
1994 Apr. 19.2	9.595	9.088	5.29	1.14–1.82	V. Good (1)	BS4027
1995 May 11.2	10.378	9.973	5.21	1.60–2.27	Good (1)	BS4345
1995 May 13.2	10.382	10.006	5.27	1.88–2.50	V. Good (3)	BS4345
1995 May 15.2	10.387	10.040	5.33	1.88–2.50	Good (3)	BS4345

^a Weighting factor used in compiling the composite spectrum.

^b Luu *et al.* (1994).

of 0.405 μm on the array. Some of the data, particularly those in the 1.2- μm region, were taken with the grating in the second order, giving $R = 383$ at 1.2 μm and spectral coverage of 0.202 μm with a single setting. The data obtained in 1995 were taken with a new InSb detector array of 256×256 pixels, giving 0.66- μm spectral coverage with a single setting of the grating in the first order. At 2.2 μm with the new array, the resolution is $R = 850$.

The wavelength calibration for CGS4 is determined from spectral lines produced by Ar and Kr lamps within the spectrometer each time the position of the grating is changed. The absolute wavelength calibration has been checked against the OH emission lines in the night sky, and the rms accuracies from quadratic fits to several lines in each spectral interval are typically 0.0001 μm . Stars of near-solar spectral type and known flux are observed at the same or comparable airmass as the target objects, with no change in the grating position. Division of the spectrum of Pholus by the stellar standard removes the effects of telluric lines and establishes the spectral flux distribution of the target object. This procedure is subject to limitations of seeing conditions and other systematic effects, such as the stability of the local water vapor content of the atmo-

sphere, which affects the ability to remove strong telluric absorption lines.

Uncertainties in the absolute flux of Pholus were primarily caused by inferior seeing conditions when the image of Pholus did not entirely fall within the slit of the spectrometer. Broadband photometric measurements (at $VJHK$ wavelengths; see Table II) were used to combine the various components of the spectrum observed over the 4-year period. JHK photometry was obtained by Davies and Sykes (1992), Davies *et al.* (1993b), and Howell (1995) (see Table II), and most recently by Davies *et al.* 1998. The photometric measurements by Howell (1995) were especially important in linking the near-infrared spectra reported here to the visible-region brightness of Pholus because she obtained JHK measurements with one telescope while V measurements were being made simultaneously with another telescope at the same observatory site. This simultaneity of the $VJHK$ measurements obviates the problems of corrections for phase angle and, especially, the brightness variation of Pholus as it rotates. We note that Davies and Sykes (1992) and Davies *et al.* (1993b) used estimated values of V for the times of their JHK observations for the calculation of the $V-J$ color. Their $V-J$ is not substantially different from that observed directly by Howell (1995), and we therefore average the two determinations by Davies *et al.* (1996) with the Howell value to obtain $V-J = 2.50 \pm 0.08$, and the other colors, as given in Table II. (Davies *et al.* (1998) find slightly different colors in their most recent paper.) In calculating the adopted average in Table II we make no corrections for phase angle because of the lack of direct information on phase-color effects for an object with the highly unusual colors of Pholus.

In order to derive the reflectance spectrum relative to 0.55 μm , the colors of the Sun were subtracted from the average $V-J$, $V-H$, and $V-K$ colors of Pholus. The solar colors used were those of Campins *et al.* (1985): $V-J = 1.12$, $V-H = 1.43$, $V-K = 1.49$. The resulting intrinsic colors of Pholus at the J , H , and K wavelengths were then converted to reflectances relative to V , for which we

TABLE II
Photometry of Pholus

UT Date (1992)	R (AU)	Delta (AU)	Phase (deg)	V	$V-J$	$V-H$	$V-K$	Source
Feb. 22.148	8.71	7.89	3.8	$17.11 \pm .07$	$2.44 \pm .07$	$2.80 \pm .08$	$2.92 \pm .06$	Howell ^a
Mar. 15.399	8.72	8.16	5.6	17.25	$2.47 \pm .02$	$2.98 \pm .02$	$2.93 \pm .02$	DTB ^b
Mar. 17.281	8.72	8.19	5.7	17.28	$2.59 \pm .02$	$2.97 \pm .03$	$2.95 \pm .02$	DTB ^b
Adopted values					$2.50 \pm .08$	$2.92 \pm .10$	$2.93 \pm .02$	

^a Published in Howell *et al.* (1992).

^b Published in Davies *et al.* (1996).

assumed $p_V = 0.06$, a value consistent with an average of the radiometric determinations mentioned above.

2.2. The Composite Spectrum

Using the available VJHK photometric points as a guide to continuum levels, we compiled the composite spectrum. Certain differences appear in the different data sets for the same wavelength interval. These include the absorption centered near $1.71 \mu\text{m}$ suggested in the Luu *et al.* (1994) spectrum and in that of Davies *et al.* (1993b); in other data sets it is not even marginally seen. Furthermore, as noted below, the Luu *et al.* spectrum shows marginal evidence for a band at $2.33 \mu\text{m}$. It is possible, perhaps likely, that as the body rotates different hemispheres of Pholus have slightly different spectral signatures, but the composite spectrum in Fig. 1 represents our best judgement in selecting and weighting the various data sets.

The composite spectrum (Fig. 1) consists of a weighted (by signal precision) average of all the data in Table I. In spectral regions of overlap between our data set and that of Luu *et al.* (1994), all of our spectra were resampled at the same wavelengths as Luu *et al.* so that averages could be computed. All spectra were taken with the same spectrometer and telescope. Large symbols in Fig. 1a represent the JHK photometry in Table II.

3. OUR MODEL

3.1. Hapke Theory

We modeled the spectrum of Pholus using the Hapke theory for diffuse reflectance from an airless planetary surface (Hapke 1993). The formulation we used has been described by Roush *et al.* (1990) and Roush (1994); in the present context we used models of intimate compositional mixes of grains and spatially segregated regions of differing composition, as described below. Calculations using the Hapke theory require the real and imaginary indices of refraction for the candidate materials to be specified, but such information is available for only a limited number of plausible components of the surface of Pholus. The limited availability of appropriate optical constants somewhat constrained our range of model computations, but we began on the assumption that specific regions of the spectrum would be most affected by specific constituents and that a final model would have to incorporate all of the components that are chemically plausible.

3.2. Tholin

We begin by matching the red slope of the spectrum from 0.4 to $1.0 \mu\text{m}$, for which we require a material rich in carbon compounds, such as the tholin organics produced by plasma irradiation of organic-rich gases. We used the

optical constants published by Khare *et al.* (1984a) for “Titan” tholin.

The material called Titan tholin is the involatile product of plasma irradiation of a gas mixture of $\text{N}_2 + \text{CH}_4 = 0.9 + 0.1$, corresponding approximately to the bulk composition of Titan’s lower atmosphere (Khare *et al.* 1984b). Titan tholin consists of a variety of C_1 – C_5 hydrocarbons and nitriles, both unsaturated and saturated (Thompson *et al.* 1991), the most abundant of which have been observed in Titan’s stratosphere by the Voyager infrared spectrometer (Hanel *et al.* 1981). Other compounds in Titan tholin include alkanes, alkenes, and nitrogen heterocyclic molecules (Khare *et al.* 1984b, Ehrenfreund *et al.* 1995). Upon acid hydrolysis of Titan tholin, some 16 amino acids are produced, with glycine the most abundant (Khare *et al.* 1986). Recent spectroscopic and chromatographic analysis of Titan tholin (McDonald *et al.* 1994) confirms earlier work demonstrating that aromatic hydrocarbons are a minor component. The water-soluble fraction of this tholin is dominated by materials of molecular weight ~ 200 – 600 amu. McDonald *et al.* (1994) quantified other compositional details of Titan tholin. Overall, the elemental composition of Titan tholin is represented by $\text{C}_3\text{H}_5\text{N}_2$ (Sagan *et al.* 1984). In our model the Titan tholin represents the complex organic solid responsible for the red color of Pholus (Fig. 2).

Qualitative inspection of the spectrum of Pholus by the authors who obtained the original data (referenced above) suggested that this tholin might match the red slope satisfactorily, and Wilson *et al.* (1994) demonstrated through their own Hapke scattering calculations that such is indeed the case. In our primary effort to model the spectral absorption features in the near-infrared, we have concentrated on other materials in addition to tholin, because while the reddish slope is explained by a tholin, neither tholins nor the other materials included in the Wilson *et al.* preferred models match the band positions, band shapes, or the albedo levels ($>1.8 \mu\text{m}$) in the new spectral data. We discuss the additional molecular components below.

3.3. Water Ice

The broad absorption band centered near $2.04 \mu\text{m}$ is well matched by absorption in solid H_2O . This band is seen in comparable strength in two other low-albedo objects, Comet 1995/O1 (Hale–Bopp) (Davies *et al.* 1995, 1997) and Saturn’s satellite Phoebe (Owen *et al.*, in preparation). Optical constants for crystalline H_2O ice at $T = 100$ K derived from measurements by Ockman (1957) (Roush 1996) were used in our calculations, although the ice on Pholus may in fact be structurally amorphous. The maximum temperature near Pholus’ equator at perihelion is ~ 118 K, while the temperature of the phase change from amorphous to crystalline (cubic) is in the range 142 – 148 K

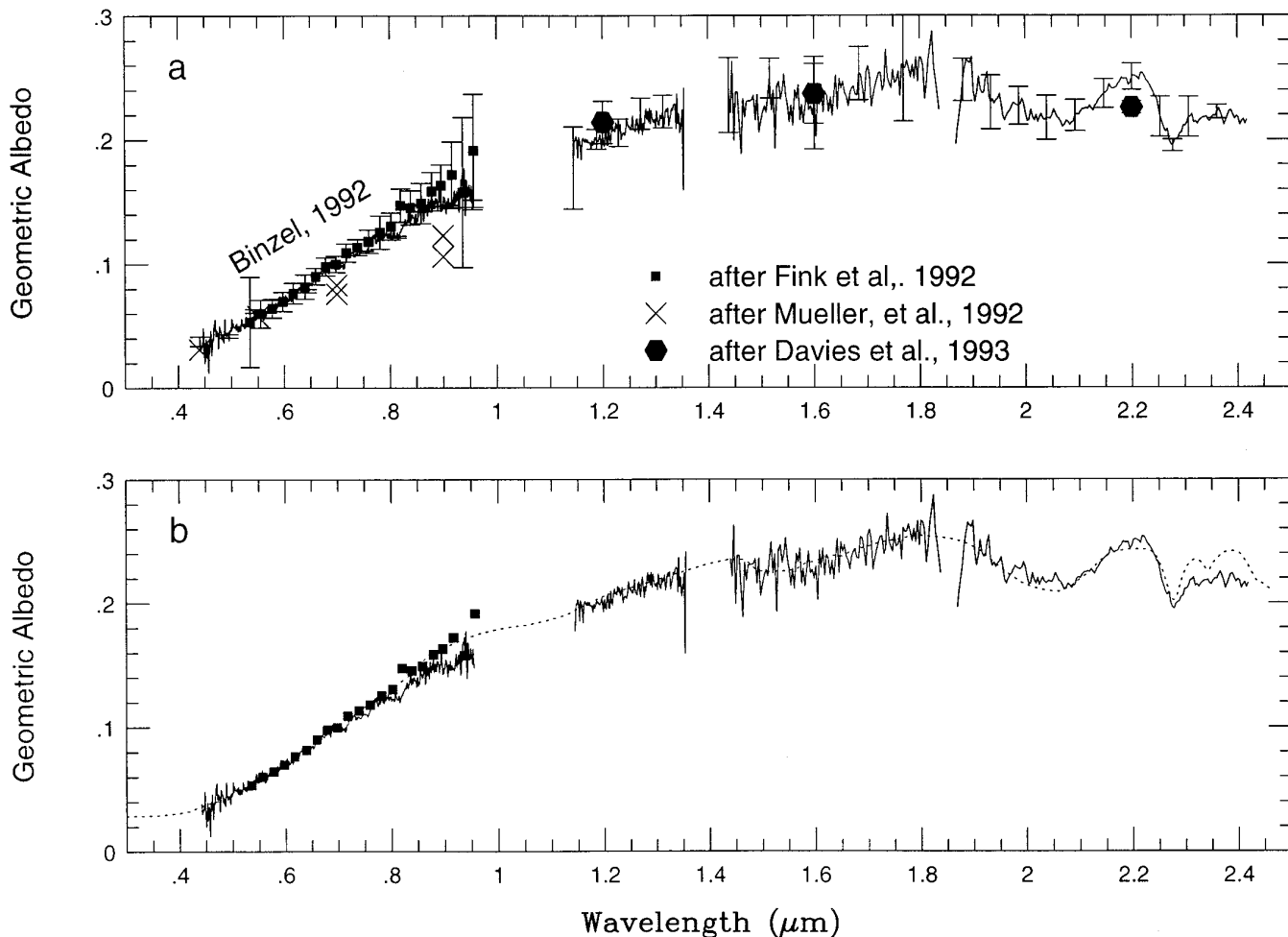


FIG. 1. This figure gives two presentations of the composite spectrum of Pholus (see text Section 2.2). (a) The composite spectrum, with representative error bars. Between 0.4 and 1.0 μm , three data sets are shown; the continuous line is from Binzel (1992), and the other symbols are identified in the key. The solid hexagons are the average values of JHK photometric points, as discussed in the text. (b) For clarity, the composite spectrum of Pholus is shown without the photometric points, error bars, or the points by Mueller *et al.* (1992). The dashed line is the model consisting of Titan tholin, olivine (Fo 82), H₂O ice, CH₃OH ice, and carbon black, as discussed in Section 3.

(Jenniskens and Blake 1996). Our data do not have adequate signal precision to distinguish clearly between the crystalline and amorphous phases; the optical constants for amorphous ice are not available in our wavelength region, so we have adopted the crystalline values for the time being.

3.4. Methanol

As an abundant molecule in interstellar space and comets, CH₃OH is an important potential component of the surface of a relatively unprocessed body such as Pholus. Because CH₃OH is a small molecule and because it is readily produced by the oxidation of CH₄, the presence of methanol is indicative of the chemically primitive nature of a surface rich in hydrocarbons.

The Pholus absorption band at 2.27 μm is matched in

position and qualitatively in shape by a band in solid methanol (CH₃OH) (Sandford and Allamandola 1993). Because CH₃OH in a vapor state has been detected in several comets (Hoban *et al.* 1991, Bockelée-Morvan *et al.* 1991, and Mumma *et al.* 1993), and because CH₃OH is observed in the solid phase in the dense cloud material toward protostars (Grim *et al.* 1991, Skinner *et al.* 1992), methanol ice is a plausible component of Pholus. Optical constants for solid CH₃OH at wavelengths shorter than 2.5 μm are not available in the literature, so we determined them from new laboratory spectra obtained in the laboratory of Dr. Vincent Anicich at the Jet Propulsion Lab. The transmission spectrum of a frozen film of 13.67 μm thickness was obtained at 90 K, and the real and imaginary indices of refraction were calculated (see Appendix

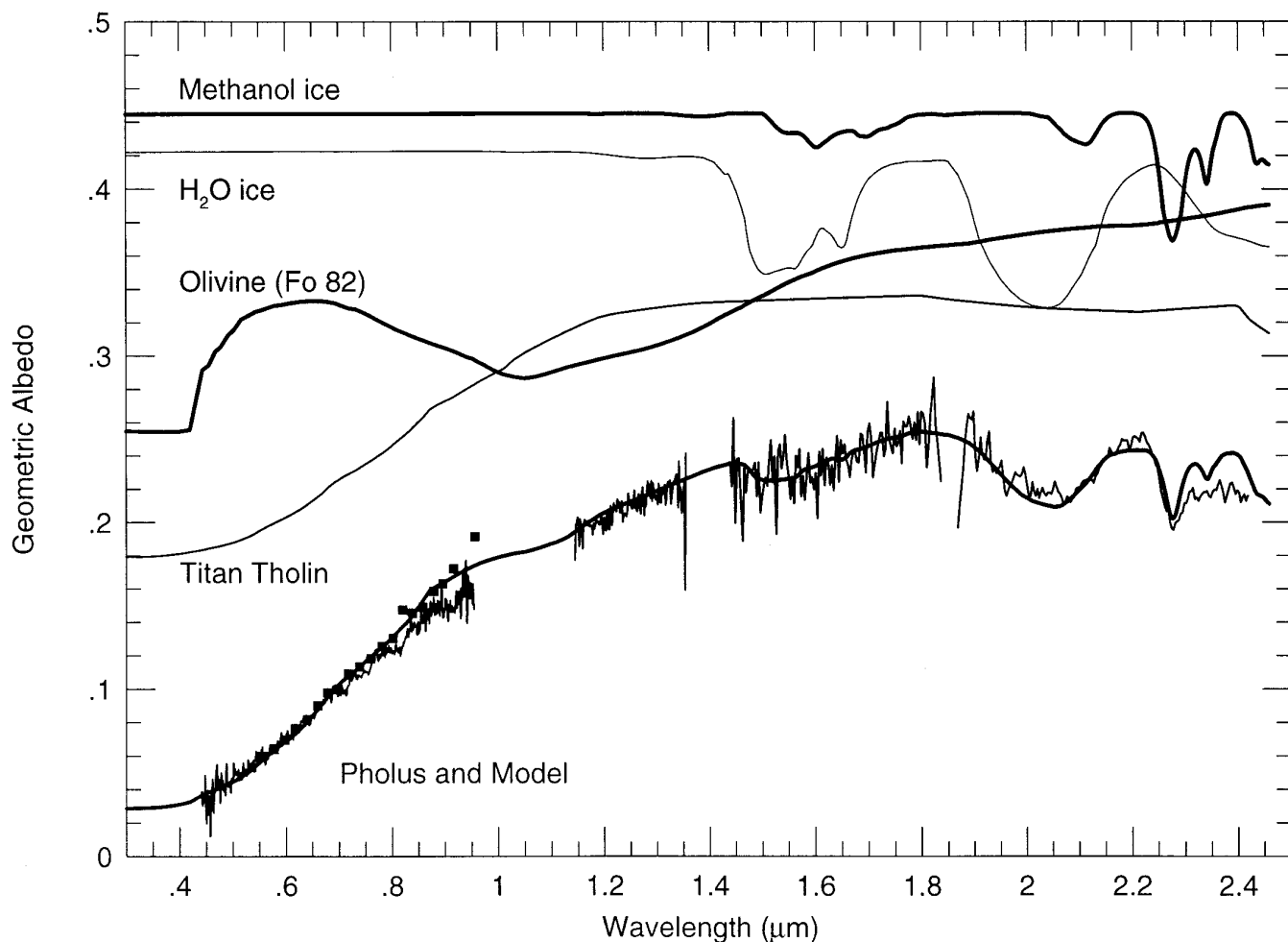


FIG. 2. The spectrum of Pholus with the model, showing the spectral contributions of each of the four principal components. The spectra of methanol ice, water ice, olivine, and Titan tholin are computed from their complex refractive indices (n, k) with the Hapke scattering model, but they are shown here with various scalings (of the ordinate) to fit them conveniently on the figure. Not shown is the neutral and featureless spectrum of amorphous carbon.

A). Figure 3 gives an overview of the solid CH_3OH spectrum.

The spectrum from which we calculated the indices for CH_3OH is in good agreement with that shown by Sandford and Allamandola (1993). In addition to the distinct band at $2.27 \mu\text{m}$, there is a weaker band in both spectra at $2.33 \mu\text{m}$ and an OH absorption centered at $2.1 \mu\text{m}$. We return later to the assignments of these bands.

Our model incorporates CH_3OH to account for the $2.27\text{-}\mu\text{m}$ band; however, methanol also has a second sharp band at $2.33 \mu\text{m}$ which does not appear in the composite Pholus spectrum. This pair of bands arises as combinations of the CH stretching and deformation modes. The many modes of CH_3OH have been identified by Barnes and Hallam (1970) for monomers, dimers, and multimers in an Ar matrix. The asymmetric stretching fundamentals lie at 3005.3 cm^{-1} (as_1 [our notation]), 2961.9 cm^{-1} (as_2), and

2956.0 cm^{-1} (as_3) cm^{-1} , with the symmetric stretch at 2847.9 cm^{-1} (ss_1). The asymmetric deformation fundamentals lie at 1474.1 cm^{-1} (ad_1) and 1465.8 cm^{-1} (ad_2), and the (weak) symmetric deformation at 1451.4 cm^{-1} (sd_1). The $2.27\text{-}\mu\text{m}$ (4405 cm^{-1}) band in our model is the combination of the asymmetric stretching and deformation ($as_2 + ad_1$, $as_2 + ad_2$, $as_3 + ad_1$, $as_3 + ad_2$), while the $2.33\text{-}\mu\text{m}$ (4292 cm^{-1}) band is the combination of the symmetric modes. The symmetric fundamental modes are characteristically weak, particularly in the deformation mode (sd_1), resulting in a significantly weaker combination band. The combinations $as_1 + ad_1$ and $as_1 + ad_2$ do not appear in the methanol spectrum.

Does solid CH_3OH exist on the surface of Pholus? In the composite spectra we present here, only the $2.27\text{-}\mu\text{m}$ band of CH_3OH is clearly visible, while the weaker $2.33\text{-}\mu\text{m}$ band is not. However, in the single spectrum of this region

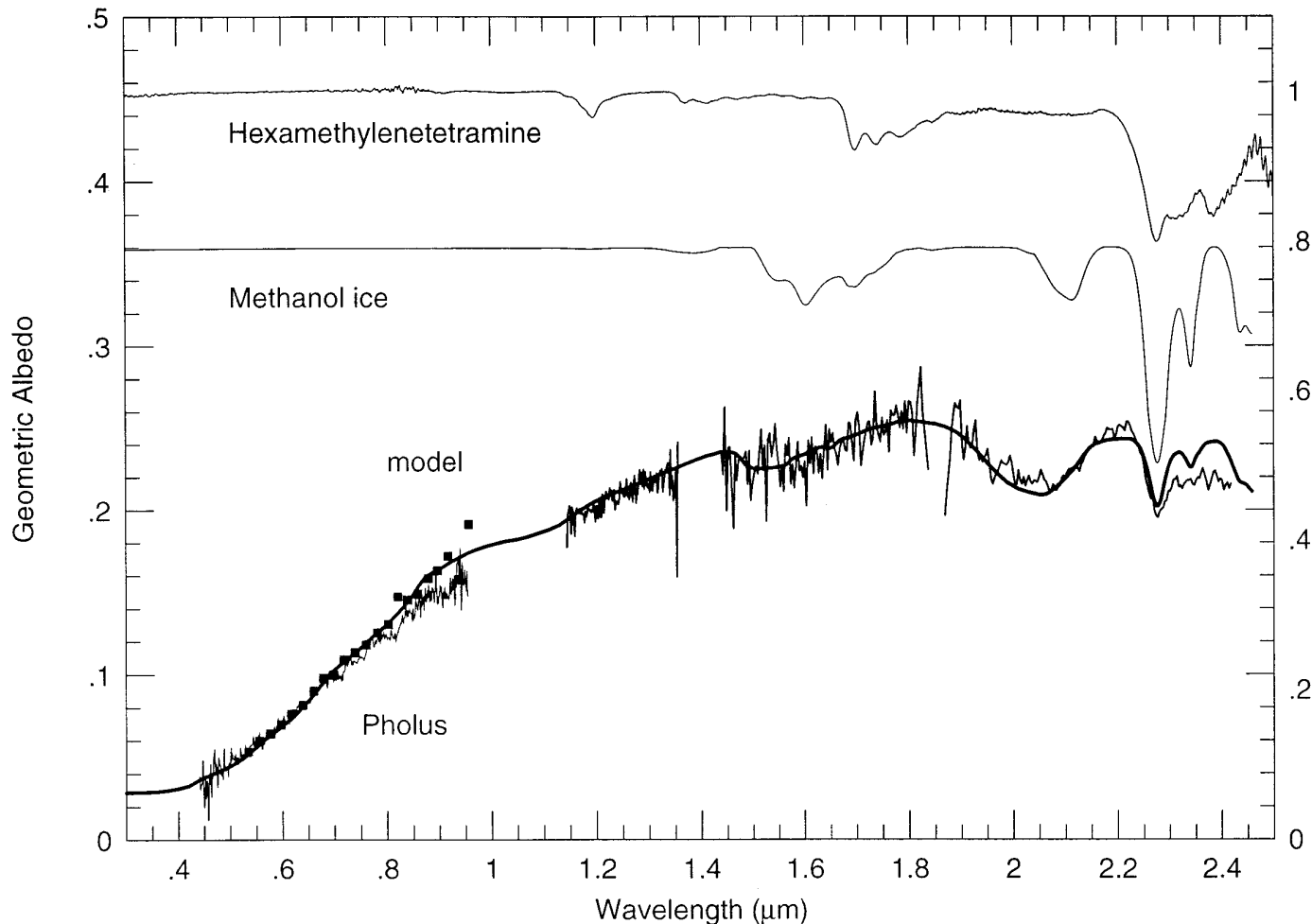


FIG. 3. The spectrum of Pholus, as in Fig. 1, and our model (ordinate on the left). Also shown are the measured reflectance spectra of powdered hexamethylenetetramine (HMT) and a computed (geometric albedo) spectrum of CH_3OH ice at 90 K ($5 \mu\text{m}$ grain size). The ordinate on the right corresponds to the HMT and CH_3OH spectra; the spectrum of CH_3OH is offset downward by 0.1 for clarity.

published by Luu *et al.* (1994), which is included in our composite, there is a suggestion of the $2.33\text{-}\mu\text{m}$ band at the level of the noise in the data. In Fig. 4 we show the Luu *et al.* spectrum and our model, which includes CH_3OH ice, for comparison.

While solid CH_3OH may occur on Pholus, in consideration of the absence of the $2.33\text{-}\mu\text{m}$ band in most of the individual spectra and in the composite, we do not claim that we have identified it uniquely in this work. We reiterate, however, that methanol is an abundant component (at the level of a few percent relative to H_2O) of at least some active comets, and the interstellar medium, both of which are probably closely related to Pholus (Greenberg 1996, 1998, Mumma *et al.* 1993, Grim *et al.* 1991). We carry CH_3OH in our models because it represents small hydrocarbon molecules, such as the photochemical products of methanol discussed in the next section, and because its

optical indices have been measured, which is not the case for other potential materials.

3.5. Nitrogen-Bearing Molecules

Spectroscopy of the dense interstellar medium (protostars embedded in interstellar gas and dust clouds [e.g., W33A]) shows the presence of ices of H_2O , CO , CO_2 , and CH_3OH , plus another band ($4.62 \mu\text{m}$) indicative of a nitrogen-bearing species, commonly referred to as XCN (e.g., Whittet and Tielens 1997, Lacy *et al.* 1984, Tegler *et al.* 1993, 1995, Pendleton *et al.* 1998). Energetic processing of mixtures of interstellar ice analogs produces a solid residue that is chemically stable at room temperature and pressure (Allamandola *et al.* 1988, Palumbo *et al.* 1998). These residues provide a good spectroscopic match to the $4.62\text{-}\mu\text{m}$ region in the spectra of embedded protostellar objects

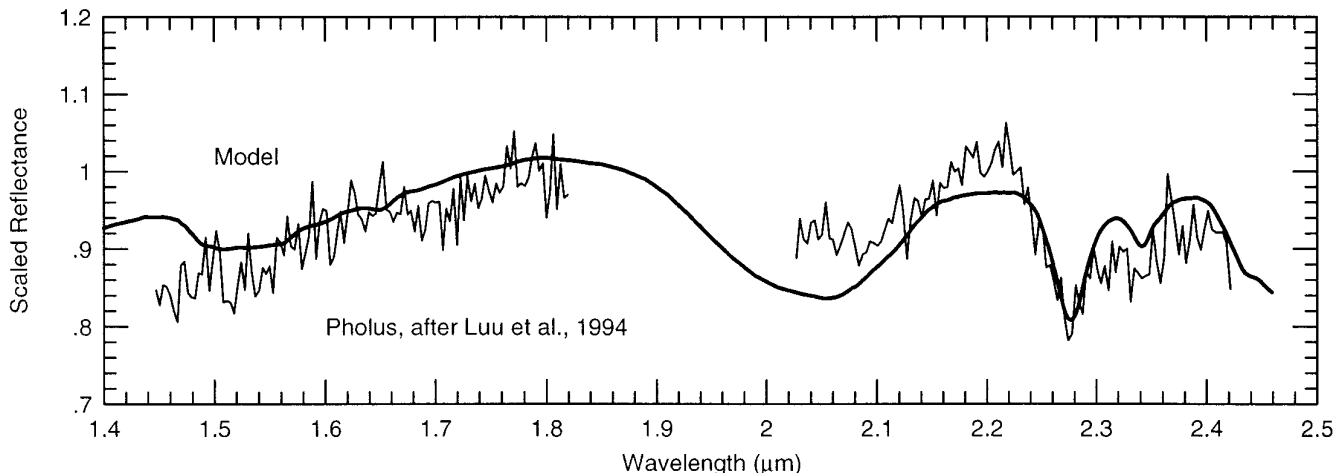


FIG. 4. The normalized spectrum of Pholus obtained by Luu *et al.* (1994), with the model presented in this paper (offset upward). Of particular note is the apparent coincidence of the two spectral absorptions due to CH_3OH (2.27 and 2.33 μm) in the model and in the Pholus spectrum, although the 2.33- μm band in the Pholus spectrum is uncertain because of the random noise (see Section 3.4).

where $\text{C}\equiv\text{N}$ stretching modes dominate (Pendleton *et al.* 1998). Ion bombardment of nitrogen-containing ices not only provides a good fit to the observational data, but also allows for the good possibility that the nitrogen is in the form of solid N_2 , as in the cases of Triton and Pluto (Cruikshank *et al.* 1998). Solid N_2 would not be broken apart by less energetic processing mechanisms, such as UV irradiation. If the nitrogen is in the form of some other molecule, such as NH_3 , which requires less energy to liberate the N, then mechanisms other than ion bombardment may be significant. Here we will focus on the UV photolysis of specific molecules, such as $(\text{CH}_2)_6\text{N}_4$ hexamethylenetetramine (HMT) as one possible scenario which could lead to the organics on bodies like Pholus. We note, however, that if data for $\lambda < 2.5 \mu\text{m}$ were available for the residue of ion-bombarded N_2 ices, that would also be an important component to investigate.

Studies of the UV-photolytic residue of irradiated $\text{H}_2\text{O}:\text{CH}_3\text{OH}:\text{CO}:\text{NH}_3$ (= 100:50:10:10) mixtures (Bernstein *et al.* 1994, 1995) show that the residue is composed of $\sim 60\%$ HMT, while the remaining $\sim 40\%$ is a mixture of ethers, amides, and ketones. HMT is potentially an important molecule because it carries four atoms of nitrogen and its synthesis incorporates NH_3 .

Bernstein *et al.* (1995) favor a synthesis mechanism for HMT in which formaldehyde, first formed by UV photolysis of methanol, reacts with ammonia to form methyleneimine (CH_2NH). This path and the subsequent reactions are shown in detail by Bernstein *et al.* (1995). The efficient conversion of NH_3 into another product, such as HMT, might also explain the low abundance of solid NH_3 in interstellar clouds ($< 5\%$, Tielens and Whittet 1997).

HMT decomposes in the presence of heat, UV irradiation, and acid hydrolysis into many cosmochemically interesting materials, including some of the original materials from which it is synthesized. Acid hydrolysis produces amino acids, ammonia, and formaldehyde, all of which are of significance in the Solar System.

We have obtained reflectance spectra of HMT in the region 0.2 to 2.5 μm at room temperature (see Appendix B). The near-infrared portion of this spectrum is shown in Fig. 3 (also expanded in Fig. 5) along with the spectrum calculated from measured optical constants for solid CH_3OH and the spectrum of Pholus. HMT has a distinct absorption band at 2.27 μm , just as does solid CH_3OH , but in place of the distinct secondary band of CH_3OH at 2.33 μm , HMT shows an absorption shoulder with minor spectral structure extending to about 2.40 μm , which is a better match to the spectrum of Pholus than is solid CH_3OH . We have not yet been able to model the Pholus spectrum rigorously using HMT because the optical constants for this material have not yet been determined in the spectral region of our data, and although HMT may eventually give a better match to the 2.27- μm region of Pholus' spectrum than solid CH_3OH , we use the refractive indices for CH_3OH in our model.

Because the photolysis of CH_3OH results in the production of formaldehyde (HCHO) as an intermediary toward the formation of HMT, and because HCHO is found in comets, we have considered the possibility that HCHO is responsible for the features seen in the spectrum of Pholus. Formaldehyde readily polymerizes to two forms, the trimer (trioxane $(\text{HCHO})_3$) and the linear polyoxymethylene $(\text{HCHO})_n$ or POM). POM was reported in the coma dust

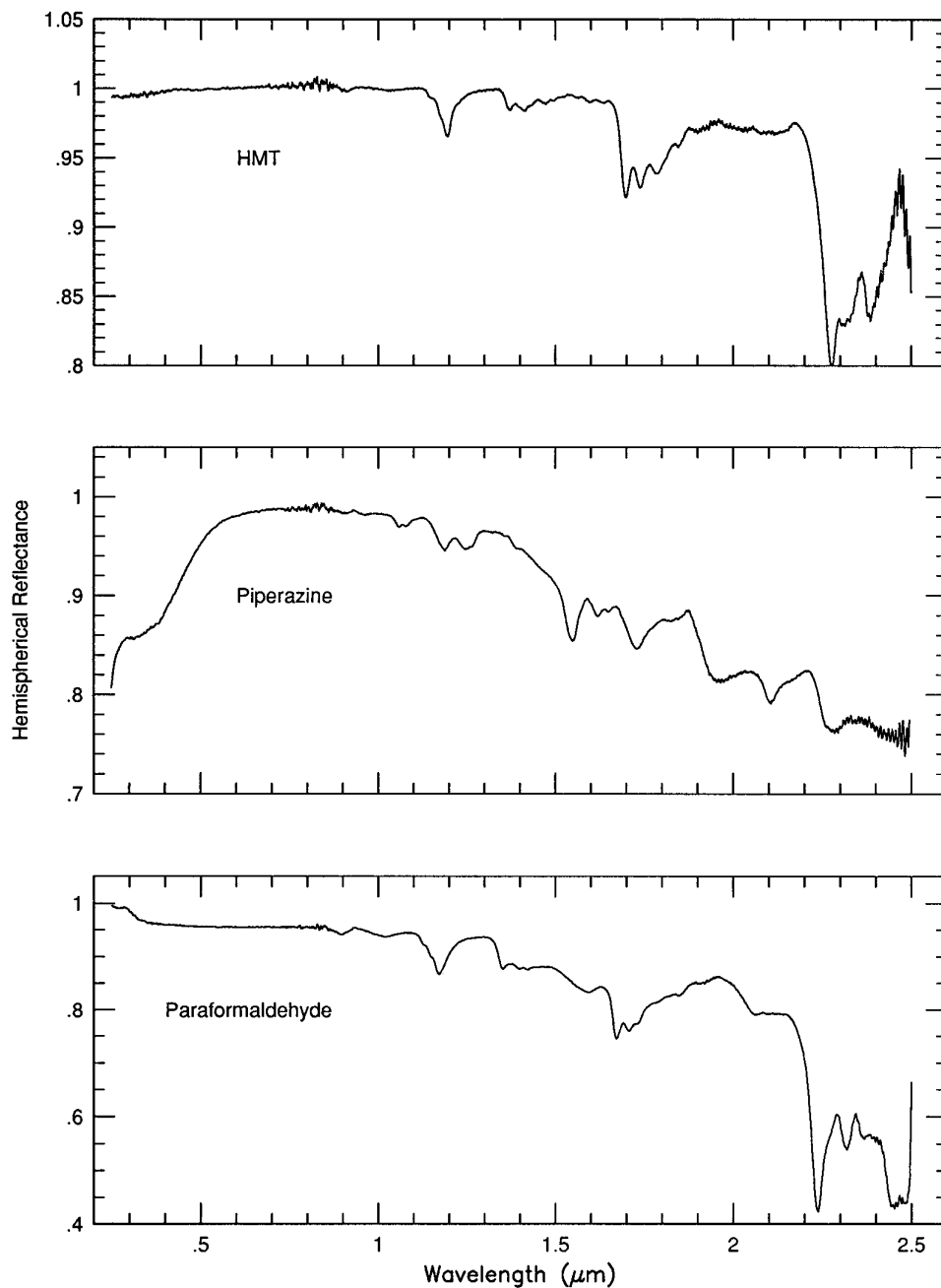


FIG. 5. Laboratory reflectance spectra of hexamethylenetetramine (HMT), piperazine, and paraformaldehyde (POM) (see Section 3.5).

of Comet P/Halley from data from the Giotto spacecraft (Huebner 1987, Mitchell *et al.* 1987, but also see Mitchell *et al.* 1992). We show in Fig. 5 our reflectance spectrum of polyoxymethylene (paraformaldehyde), which shows structure in the 2- to 2.5- μm region, but which does not match the structure in the spectrum of Pholus. We show it here for completeness.

The chemical evolution of methanol appears to depend

upon the nature of the irradiation (UV or ion bombardment). When an ice mixture of H_2O and CH_3OH is bombarded with ions it produces acetone [$(\text{CH}_3)_2\text{CO}$] (Strazzulla *et al.* 1995) instead of formaldehyde. If NH_3 were to be included in the mixture, HMT would not form but other nitrogen containing molecules might arise. As a representative of these, we have included in Fig. 5 piperazine, an amine similar in structure to trioxane, with a 1- to 2.5- μm

spectrum similar to HMT. If N₂ were included in the mixture, UV photolysis would not break the N–N bond, but ion bombardment would. In the case of the interstellar medium, the energy source involved in nitrogen chemistry is not yet known, but the outcome of ongoing investigations may affect the conclusions eventually reached about the nitrogen in comets and on Pholus.

3.6. Minerals

Our model incorporates 20- μm grains of olivine to account for absorption in the 0.9- to 1.3- μm region in the spectrum of Pholus. Without this component, the model composed of tholin, H₂O, and CH₃OH ices, and elemental carbon shows a large departure from the data between 0.9 and 1.3 μm ; olivine brings the model and the data into excellent accord. We used the optical constants of forsterite (Oahu Island olivine, Fo (82)), derived by Pollack *et al.* (1994) from data of Hiroi and Takeda (1990). Other olivines with different Mg and Fe contents can also fit the Pholus spectrum, but the abundances will be different.

The strength of the 1.1- μm band complex (and to some degree its exact central wavelength), depend upon the relative Mg and Fe contents; the high-Mg forsterite bands are weaker than in the high-Fe fayalite olivine (e.g., Lucey 1998). We have chosen the forsterite Fo (82) because current indications are that the olivines in both comets (Crovrier *et al.* 1997, Schulze *et al.* 1997) and in the interstellar grains (Waters *et al.* 1998) are Mg rich. Choice of another olivine with higher Fe content would reduce the amount required to match the observed absorption on Pholus.

We considered minerals as a possible source of the 2.27- μm feature. Reflectance spectra of 10 minerals having relatively narrow spectral features in the 2.2- to 2.4- μm region are given by Bell *et al.* (1994, Fig. 7), and we have further examined the spectra of nine chlorites and perchlorites in the USGS Digital Spectral Library (Clark *et al.* 1993). We found no plausible minerals that have the 2.27- μm Pholus band with the correct central wavelength and bandshape. Although there may be other minerals not examined by us that have a spectrum similar to that of Pholus in the near-infrared, we do not pursue this possibility further and return our focus to volatiles and hydrocarbons.

3.7. Low-Albedo Component

The three components discussed so far have high albedos when seen in diffuse reflectance, while the surface of Pholus has a very low albedo in visible wavelengths. Therefore, we have introduced into our models a fourth component to lower the albedo to match that of Pholus. We use carbon black, a form of elemental carbon that has very high absorption across the visible and near infrared spectrum and is quite neutral in color.

3.8. Our Model Fit

The best model fit to the data was found by a manual iterative technique, in which the principal effects of each molecular component were first evaluated, individually and in an ensemble, and then applied. Our best-fitting model of the Pholus spectrum consists of two principal components. The first is an intimate mixture of 55% olivine (Fo 82) in 20- μm grains, 15% Titan tholin with grain size 1 μm , 15% H₂O ice with grain size 10 μm , and 15% CH₃OH ice with grain size 10 μm . Within this intimate mixture of the four grain types, an incident photon encounters all four kinds of grains before leaving the surface. The second principal component is carbon black. The two components are modeled together as a spatially segregated mixture, that is in a checkerboard kind of pattern; a photon scattering from one component does not strike the other before leaving the surface. The best-fitting mixture of the two principal components required to achieve the albedo of Pholus at every wavelength is 61.5(\pm 5)% carbon black and 38.5 \pm 5% of the olivine–tholin–water–methanol mixture. We note that the compositional model reported here represents the surface of Pholus and may not be reflective of the bulk composition.

We found that in order to achieve the steep red slope at the correct albedo level in the visual spectral region, tholin grains of 1 μm were required. This small size violates the principle adopted for Hapke scattering models that the grain size must be at least three times the wavelength (in the same units). There are several ways to increase the particle sizes we use. One is to scale the optical constants of the tholin to retain the visual slope but to be less absorbing. This would likely result in larger abundances of tholin contained in the mixtures. Another approach would be to increase the internal scattering within particles; this would have the net effect of increasing the grain diameters for all components. Instead of taking either of these *ad hoc* approaches, we simply note that the tholin grain size violates certain conditions associated with Hapke theory.

4. OTHER MODELS

4.1. The Wilson *et al.* Model

Wilson *et al.* (1994) and Wilson (1997) used Hapke scattering theory to compute a synthetic spectrum to match that of Pholus. They used optical constants of ices and hydrocarbons in various combinations for a hypothetical material that would match the red color (0.4–1.0 μm). They concentrated their study on the photovisual spectral region, using the same data presented here (Fink *et al.* 1992, Mueller *et al.* 1992, Binzel 1992). Their study incorporated the original near-infrared spectrum by Davies *et al.* (1993b), and their models were fit to that data set. Using

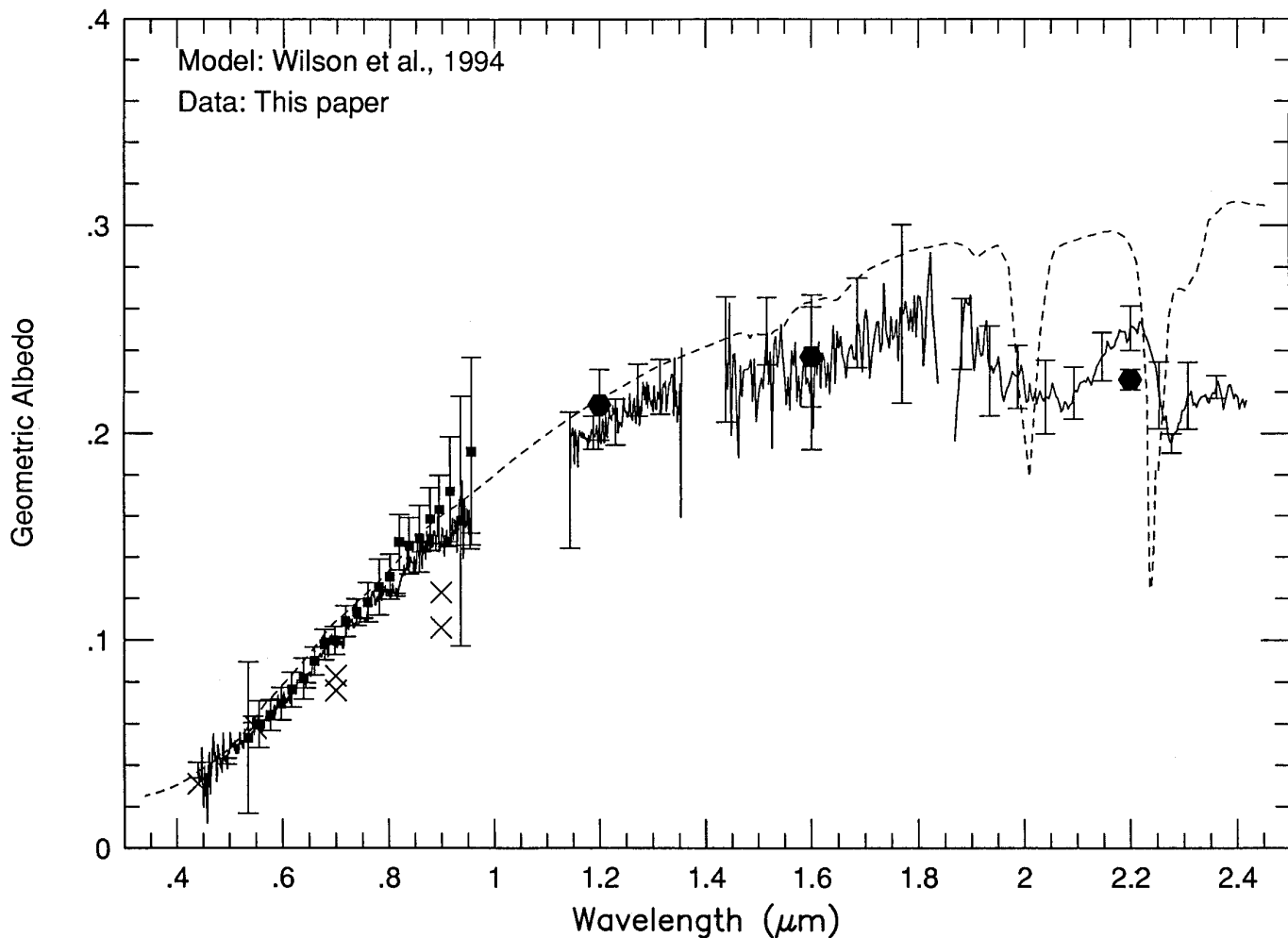


FIG. 6. The composite spectrum of Pholus presented in this work, with our computation of the Wilson *et al.* (1994) model (see Section 4.1).

the real and imaginary refractive indices of a variety of individual materials, they sought mixtures (termed intraparticle mixtures) of these materials that, when the individual n and k values of which were added in a linear way, would reproduce the hypothetical bulk material matching the spectrum of Pholus that they derived from the sources noted above.

We note that Wilson *et al.* used refractive indices of H_2O ice from Warren (1984), which are for ice at $T \sim 269$ K, whereas in our models we use indices for ice at the more appropriate temperature $T = 100$ K, as noted before. Although the differences in the indices are slight, there is a small shift to longer wavelengths of the ice band centers and a narrowing of the bands with decreasing temperature.

Wilson *et al.* favored two intraparticle mixtures. One mixture (HTW) consists of 0.15 Titan tholin, 0.1 hydrogen cyanide polymer, and 0.75 H_2O ice (particle size $10 \mu\text{m}$). The second model (HTA), giving a better fit to the spectrum, consists of the same components except that NH_3

ice is substituted for H_2O and a pure hydrocarbon tholin (having no nitrogen) is substituted for the Titan tholin.

In Fig. 6 we reproduce the best of the two preferred Wilson *et al.* models (HTA) for comparison with our newly derived spectrum in the near-infrared and the three previously published data sets in the photovisual spectral region. For Fig. 6 we have recalculated the model from the Wilson *et al.* HTA recipe in terms of geometric albedo, whereas Wilson *et al.* worked with normalized brightness. The discrepancies between the model and the data arise for $\lambda > 1.4 \mu\text{m}$ and are particularly evident in the mismatch between the strong NH_3 absorption bands (2.01 and $2.24 \mu\text{m}$) and the broader absorption bands in Pholus' spectrum at nearby but somewhat different central wavelengths.

We find no evidence for NH_3 in the spectrum of Pholus.

4.2. The Hoffmann *et al.* Model

Hoffmann *et al.* (1993) calculated Hapke scattering models using Titan tholin (grain size $3 \mu\text{m}$) and neutral colored

materials of high and low albedo. They found a satisfactory match to the spectrum of Pholus by Fink *et al.* (1992), 0.4–1.0 μm , but did not consider the near-infrared region. Wilson *et al.* (1994) discuss the Hoffmann *et al.* model in the context of their preferred mixtures, and we do not consider the Hoffmann work further here, because our emphasis is on the near-infrared region, and neither the Titan tholin (alone) nor neutral materials match that portion of the spectrum.

4.3. The Asphaltite Model

On the basis of laboratory spectra of a suite of natural terrestrial organic solids by Cloutis (1989) and Moroz *et al.* (1991, 1992), Cruikshank *et al.* (1993) proposed that the red color and the 2.27- μm absorption band of Pholus might be matched by similar features shown by those materials. The solids studied were tar sands, asphaltite, kerite, anthraxolite, etc., all containing varying amount of solvent-soluble hydrocarbons of low to medium molecular weight (<500 amu), collectively called bitumen. In his search for diagnostic spectral features for remote sensing of organic solids on Solar System bodies and on Earth, Cloutis (1989) identified near-infrared absorption bands in natural tar sands with specific overtones and combinations of C, H, and O vibrational fundamental modes. Tar sand contains macromolecular organic material that is related to petroleum.

The most familiar macromolecular carbon material is kerogen. Kerogen is the fraction of organic matter which is insoluble in the usual organic solvents and is frequently referenced in connection with meteorite and asteroid organics (e.g., Cruikshank and Kerridge 1992, Cronin *et al.* 1988, Cloutis *et al.* 1994). In a terrestrial setting, where organic solids result from thermal processing of the decay products of biological activity, kerogens are members of the sequence of natural terrestrial carbonaceous materials representing a continuous sequence from oil to graphite. The sequence is distinguished in large part by the changing ratio H/C; oil has the highest H/C, while graphite is pure C. Asphaltites (H/C 1–1.6), kerites (H/C 0.6–1.4), and anthraxolites (H/C 0.03–0.1) are solid nongraphitic members of this sequence, with anthraxolite being essentially the equivalent of kerogen. The degree of aromaticity (predominance of carbon ring structures) increases with decreasing H/C, ultimately terminating in the hexagonally structured graphite, devoid of hydrogen.

Asphaltite, kerite, and tar sand show a strong absorption band centered at 2.285 μm with a profile similar to that of the 2.27- μm band of Pholus. The mismatch in wavelength is too large to explain in terms of temperature or minor compositional effects. Thus, we abandon for the present time the proposal by Cruikshank *et al.* (1993) of a strong compositional similarity.

The comparison of terrestrial organic solids with bodies in space retains considerable value; a coal model of the interstellar extinction by Papoular *et al.* (1989, 1993a,b) is of interest because it provides a fit to the ultraviolet interstellar extinction curve and other spectral regions in the infrared. As noted before, reflectance spectra of suites of asphaltites, kerites, and anthraxolites show color characteristics similar to those of the low-albedo asteroids of the C, P, and D classes (Moroz *et al.* 1991, 1992), even though the strong band in many of these materials at 2.285 μm does not fit the Pholus spectrum. Low-albedo asteroids show no distinct absorption bands between 1 and 2.5 μm (e.g., Luu *et al.* 1994, Barucci *et al.* 1994, Owen *et al.* 1995)².

In the photovisual spectral region, as Moroz *et al.* (1991, 1992) and Cloutis *et al.* (1994) found, the presence of both aliphatic and aromatic groups is needed to give the red colors of the asphaltite-like organics, but variations in the exact shape and slope of the reflectance spectra of these materials are to be expected in materials that are inherently complex mixtures of diverse composition and structure. Recall that Titan tholin consists of mostly aliphatic hydrocarbons.

5. DISCUSSION

5.1. Organics on Pholus

We assert in this paper that the surface of Pholus is rich in complex carbon compounds represented here by a specific tholin, and we show spectral evidence that small, light hydrocarbons, methanol and/or its photolytic products, as well as H₂O ice, occur on the exposed surface. This mix of complex and lighter organic molecules has two basic sources. First, about one-half of the interstellar dust in the molecular cloud from which the Solar System formed consisted of carbon and organic-rich grains, if that molecular cloud was typical of others in the Galaxy (Tielens and Allamandola 1987). Second, after the formation of Pholus as a solid planetesimal, irradiation by ultraviolet photons, solar wind particles, and cosmic rays continued to affect the organic chemistry of the upper several meters of the crust or regolith. A third, though less significant, potential

² Cruikshank *et al.* (1991) reported absorption bands in some asteroids, the dark hemisphere of Iapetus, the rings of Uranus, and two comets, and proposed the identification of the CN bond in solid organic materials. The astronomical data were drawn from various published and unpublished sources. Since the publication of that paper, spectra of higher quality of the same (and other) asteroids (Luu *et al.* 1994, Barucci *et al.* 1994) and the dark hemisphere of Iapetus (Owen *et al.* 1995) have shown that the apparent absorption bands in the earlier data were spurious. The two comets, Panther (1981 II) and Bowell (1982 I), cannot be observed again, so the published spectra by Jewitt *et al.* (1982), which appear to show a strong absorption band at 2.26 μm , must be considered valid. The reality of an absorption band in the rings of Uranus remains ambiguous.

source arises from the interaction of Pholus with organic and other material in the interstellar medium, including other giant molecular clouds, as the Solar System moved through the Galaxy for 4.5 Gy.

Concerning the material from which Pholus condensed, there is growing evidence from comets, meteorites, and interplanetary dust particles that much of the original organic matter in the outer solar nebula was retained during the planetesimal building phase of the Solar System's origin, and that much of the incorporated material survived without melting or vaporization (Bradley *et al.* 1997, Bernatowicz 1997, Cruikshank 1997). Thus, Pholus began with an abundant inventory of complex organic molecules that resided on the interstellar grains from which it formed. The nature of the organic matter from which Pholus formed is revealed by the dust in the interstellar medium, particularly that material in the dense molecular clouds. The dust component of the clouds consists of a mix of silicate grains and grains of organic solids composed of refractory material (polycyclic aromatic hydrocarbons, photolytic residues such as $(\text{CH}_2)_6\text{N}_4$ and HCHO , etc.), and volatile ices of H_2O , CO , CO_2 , alkanes, CH_3OH , OCS , H_2 , XCN , etc. We find both organic material and a silicate on Pholus.

5.2. Processing of Surface Materials

Among those processes affecting the chemistry of Pholus after its formation, we consider only solar heat, the ultraviolet solar radiation and the flux of galactic cosmic rays (GCR); the solar wind was likely to have been blocked by the heliopause, if Pholus' original position in the Kuiper Disk was beyond about 50 AU.

Solar ultraviolet at the heliocentric distances of bodies in the Kuiper Disk is weak (for $\lambda \leq 1500 \text{ \AA}$, the flux is $\sim 10^{-3} \text{ erg cm}^{-2} \text{ sec}^{-1}$), but the time scale is long; in 4.5 Gy $\sim 1.5 \times 10^{14} \text{ erg cm}^{-2}$ was deposited. Energetic processing is clearly capable of inducing chemical changes in organics and in ices. The details of the changes depend upon the radiation source (UV, ions, particles, etc.) and exposure time, the ice composition, temperature, etc., but the basic process involves the break-up of individual molecules into fragments that recombine to form more complex molecules and polymers. The resultant materials have strong charge-transfer electronic bands that absorb most in ultraviolet, but extend to visible wavelengths. Hydrogen is removed during the irradiation, and the end state is a mass of macromolecular carbon that is depleted of hydrogen. Titan tholin is produced initially in this way (corona discharge) from a mixture of gases, but the chemical processing is grossly similar to that in an ice, and the tholin is an intermediate step in the production of what, with continued irradiation (especially with a higher energy component), would become mostly carbon (Khare *et al.* 1989, 1993). In this sense, the extended irradiation processing of hydrocarbon ices is

somewhat similar to the thermal processing of terrestrial biological matter toward oil, kerogen, and graphite. The principal difference is that the laboratory experiments produce mostly aliphatic organics and complex polymers, while natural terrestrial organics are dominated by aromatic structures.

Aliphatic hydrocarbons have been found along several different sightlines through the diffuse interstellar medium in our Galaxy (Sandford *et al.* 1991, Pendleton *et al.* 1994) and are possibly produced in the outflow stages of late-type stars (Geballe *et al.* 1998, Chiar *et al.* 1998). The availability of these materials for incorporation into newly forming planetary systems makes them important in this study. The remarkable similarity of the aliphatics in the diffuse ISM to the Murchison meteorite (Pendleton *et al.* 1994) underscores this possibility.

Once incorporated into the planetesimals, surface processing must continue over the 4.5 Gy of the Solar System. Even with generous estimates of surface overturn through impact gardening of Pholus' surface, there was ample time and radiation to effect surface organic chemistry by solar ultraviolet light and to a depth characteristic of the small-scale impact gardening process. Experience with ultraviolet irradiation of carbon-bearing ices in the laboratory (e.g., Thompson *et al.* 1987) shows that as the radiation dose increases, an initially neutral-colored and high-albedo ice becomes red as the violet albedo decreases. Further irradiation gradually reduces the albedo at all wavelengths, and ultimately the material becomes very dark, neutral in color, and spectrally featureless.

Galactic cosmic rays (GCR) have their maximum flux in the energy range 10 MeV to 10 GeV. The total energy deposition will be about $9 \times 10^{-3} \text{ ergs cm}^{-2} \text{ s}^{-1}$, or $1.3 \times 10^{15} \text{ ergs cm}^{-2}$ over the age of Solar System. For 1 GeV GCR, the deposition of the energy will occur over about the upper 10 m of surface (depending upon the density), for an accumulated flux of $1.3 \times 10^{12} \text{ ergs cm}^{-3}$. The efficiency of production of complex molecules is about $1 \times 10^{-3} \text{ eV}^{-1}$ (Schutte 1988). Using this efficiency factor, and following the model for production of the complex organic molecules ($>50 \text{ amu}$) in the crust and interior of Comet P/Halley (Mitchell *et al.* 1992), in 4.5 Gy, the number fraction of these molecules relative to H_2O is ~ 0.1 at the surface and ~ 0.0005 at a depth of 100 m. Mitchell *et al.* (1992) observed $\sim 10^{-3}$ complex molecules per H_2O in the coma dust of P/Halley, and reasoned that production of these molecules by GCR after the accretion of the comet's nucleus was insufficient to account for this number density. The complex molecules therefore were included in the material from which the nucleus accreted.

The same reasoning pertains to Pholus and other planetesimals still in the Kuiper Disk and the Oort Cloud; their organic inventory was largely set by the material from which they accreted, and although it has been altered to

some depth by the GCR flux in 4.5 Gy, the basic inventory has not changed.

What, then, causes the difference between Pholus and the low-albedo asteroids and comets in the inner Solar System? The only remaining known factor, after UV and GCR are accounted for, is the ambient heat provided by the present Sun and the heating events in the inner Solar System from the early Sun. The presence of differentiated asteroids and the hydrothermal chemical alteration of other asteroids, all revealed in the meteorite record, demonstrates the reality of those early heating events, although the exact physical causes continue to be debated. In any event, objects in the Kuiper Disk did not experience the heating experienced by objects in the inner planetary zone.

Do other Solar System bodies show evidence for organic solids? Both Triton and Pluto have solid CH₄, and the low albedo material that darkens portions of their surfaces may be refractory complex organic matter (Cruikshank *et al.* 1997, 1998). McCord *et al.* (1997) have reported spectral evidence (at 3.4 μm) from the Galileo spacecraft for spatially isolated deposits of organic material on Ganymede and Callisto. The dark hemisphere of Iapetus (Owen *et al.*, in preparation) shows both a red color and a strong absorption band at 3 μm attributed to tholin in combination with H₂O ice. Near-infrared spectra of the Kuiper Disk object 1993 SC (Brown *et al.* 1997) shows strong absorption bands bearing similarity to the spectrum of Triton, but with notable differences. The presence of hydrocarbons (perhaps CH₄) is strongly indicated on 1993 SC (Brown *et al.* 1997).

The low albedo and neutral or red colors (0.3–1.5 μm) of comets and certain classes of asteroids (C, P, and D) have long been thought to indicate the presence of macromolecular carbon-bearing molecules in their surface materials (e.g., Cruikshank 1987, 1989, Owen *et al.* 1995), but they do not show spectral absorption features diagnostic of the composition of those carbon-bearing molecules. In particular, the band we see in the Pholus spectrum at 2.27 μm is not seen in any other plausible candidate object to date (e.g., Luu *et al.* 1994, Barucci *et al.* 1994). It is reasonable to conclude that the organic signatures in the nuclei of comets and the surfaces of C, P, and D asteroids have been removed by heating and devolatilization, leaving very large molecules (>500 amu) and elemental carbon, both of which have very high opacity and no diagnostic spectral bands when seen in diffuse reflectance in the accessible spectral regions.

5.3. Other Objects

Low-albedo asteroids at Jupiter's heliocentric distance (the Trojans) and in the asteroid Main Belt, have colors (0.5–2.5 μm) that are either neutral (flat), or red to varying degrees (e.g., Luu *et al.* 1994, Barucci *et al.* 1994). However,

none of the reddest asteroids are even approximately as red as Pholus (Mueller *et al.* 1992). Similarly, the colors of comets in various stages of activity are never as red as Pholus (Hartmann *et al.* 1986, Mueller *et al.* 1992, Jewitt and Meech 1988, Luu 1993). The colors of a number of Kuiper Belt objects are comparably red to Pholus (Tegler and Romanishin 1998, Jewitt and Luu 1998).

The Centaur 7066 Nessus (1993 HA₂) has an orbital similarity to Pholus, with perihelion beyond Saturn and aphelion inside Pluto's orbit, suggesting a similar origin and dynamical history. Nessus is somewhat fainter than Pholus, but only slightly less red in color (Davies *et al.* 1996, 1998). The Davies *et al.* (1998) colors of Nessus, which can be compared with the Pholus photometry in Table II, are $V-J = 2.29 \pm 0.04$, $V-H = 2.57 \pm 0.1$, and $V-K = 2.57 \pm 0.1$. Spectroscopy of Nessus in the near-IR has not yet been achieved, but its color and dynamical similarities to Pholus invite speculation that its surface is also rich in primitive organic molecules.

Centaur 2060 Chiron, which has an orbit similar to that of Pholus, has a coma of variable intensity (Hartmann *et al.* 1990, Meech and Belton 1990) and a low-albedo, spectrally featureless continuum reflectance out to 2.5 μm (Luu *et al.* 1994). The spectrum (1.4–2.4 μm) of Centaur 1997 CU₂₆ (Brown *et al.* 1998), which crosses the orbit of Uranus, shows clear evidence of H₂O ice, but no other absorption bands. Thus, Centaurs appear to fall into at least three compositional classes, of which Chiron, Pholus, and 1997 CU₂₆ are the defining examples. Jewitt and Luu (1998) report a range in colors among the Kuiper Belt objects and the Centaurs, including some as red as Pholus. Tegler and Romanishin (1998) define two distinct color classes (neutral and red) for the Centaurs and Kuiper Belt objects; the diversity among these objects appears to be greater when the spectra are examined.

6. CONCLUSIONS

The extraordinary red color and the rich near-IR spectral signature of Pholus are explained by the presence of the common silicate olivine, a refractory solid complex of organic molecules (tholin), ices of H₂O and CH₃OH (or a similar molecule), and carbon on its surface. The red color of Pholus is thus thought to have been produced by the energetic processing (solar ultraviolet, corona discharge, or ion bombardment, alone or in some combination) of simple molecules (CH₄, H₂O, CO, NH₃, N₂, CH₃OH). The photolytic products of these simple molecules are larger molecules ($\leq \sim 300$ amu) which are relatively refractory and stable, but which upon further irradiation would continue to reduce to elemental carbon and macromolecular carbon-bearing molecules (>500 amu) in the presence of significant heating. We propose that most of the organic material on Pholus' surface represent the *partially pro-*

cessed remnants of the original inventory of material, formed in the interstellar medium, from which Pholus and other planetesimals accreted in what is now the Kuiper Disk.

Further processing of Pholus by solar UV and heat can be expected to remove hydrogen from the small organic molecules, transforming the surface into a less red-colored and spectrally featureless macromolecular carbonaceous mass. By this reasoning, Chiron represents the more heavily processed stage of the chemical evolution of such a body.

Insofar as the reflectance spectrum of Pholus is so well fit by a rigorous model that includes all of the basic components of comets, it seems reasonable and appropriate to think of Pholus as the nucleus of a comet that has never been active. As such, it is demonstrably one of the most primitive objects yet studied.

APPENDIX A: THE METHANOL SPECTRUM

Laboratory measurements of the spectrum of solid methanol were made at the Extraterrestrial Ice Facility, at the Jet Propulsion Laboratory. Spectra were measured between 1 and 5 μm at temperatures between 90 and 120 K, a range which includes the temperature at which a solid phase transition occurs.

A thin film of methanol was formed by spraying gaseous methanol onto a sapphire window, held at $T = 90$ K, at a rate of approximately 0.07 $\mu\text{m}/\text{min}$. The exact thickness of the film was determined by measuring interference fringes produced by a laser whose beam was directed onto the area where the film was forming. The film thickness for the measurements presented here was 13.67 μm .

The temperature of the window was maintained by a combination of cooling, provided by contact with a cold finger, and warming, from a heater, attached to the window. The temperature of the window was known to an accuracy of ± 0.5 K during the measurements.

A spectrum was taken at 90 K, and then the temperature of the system was incrementally raised to 120 K. Spectra taken at intermediate temperatures show that a change in the shape of some of the spectral bands occurred between 100 and 105 K, probably corresponding to a phase transition of solid methanol that occurs in this temperature range (Falk and Whalley 1961).

Values of the real and imaginary indices of refraction were determined by using the subtractive-Kramers-Kronig analysis (e.g., Warren 1984).

APPENDIX B: THE LAB SPECTROMETER

Experimental measurements of the spectral reflectance of our laboratory samples in the 0.25- to 2.5- μm region were made at room temperature using a dual-beam, dual-monochrometer, dispersive Perkin-Elmer Lambda 9 UV/VIS/NIR spectrophotometer equipped with a Labsphere DRTA-9 integrating sphere. The integrating sphere is coated with Spectralon, a high reflectance material (the spectral reflectance is greater than 95% over the entire wavelength region), and disks of the same material were used for the reference beam and the instrument background correction. The 6-inch-diameter sphere has entrance ports to admit the sample and reference beams.

The sample is positioned opposite the entrance port to make reflectance measurements in an integrating sphere. The light scattered into all angles of the backward hemisphere is collected by the sphere and measured by the detector after multiple internal reflections. Internal reflections against

the diffuse surface of the integrating sphere average out the surviving angular components of the scattered or reflected light before it reaches the detector.

The measured reflectance data could be corrected to obtain the absolute reflectance of the samples. This small correction factor, the diffuse spectral reflectance of the coating material, accounts for absorption of the integrating sphere's coating material at the reference beam reflectance port. However, data provided by the manufacturer indicate that the reflectance of the coating material is greater than 96% at all measurement wavelengths, so this correction is negligible at most wavelengths, ranging to at most a 4% decrease in reflectance at the wavelengths where the coating is most highly absorbing.

ACKNOWLEDGMENTS

We thank Dr. Jane Luu for providing a digital version of the spectrum of Pholus from Luu *et al.* (1994), and Dr. L. V. Moroz for her contributions to an early draft of this paper. Dr. Scott Sandford kindly provided a near-IR spectrum of frozen methanol and together with Dr. L. J. Allamandola gave us helpful comments. Dr. Ellen Howell kindly made available her photometry of Pholus in advance of publication. Dr. Vincent Anicich made available his laboratory facilities for the measurement of the spectra of several materials used in this work. Dr. R. Binzel provided a copy of his spectrum in digital form. We thank Dr. G. H. Herbig for a discussion of the accretion of interstellar dust particles on Pholus. We are grateful to the staff of UKIRT for its excellent support of the telescope and CGS4. This research is supported by NASA through Planetary Astronomy RTOP 196-41-67-03, Planetary Geology and Geophysics RTOP 151-01-60-01, and other sources.

REFERENCES

- Allamandola, L. J., S. A. Sandford, and G. J. Valero 1988. Photochemical and thermal evolution of interstellar/precometary ice analogs. *Icarus* **76**, 225–252.
- Barnes, A. J., and H. E. Hallam 1970. Infrared cryogenic studies. 4. Isotopically substituted methanols in argon matrices. *Trans. Faraday Soc.* **66**, 1920–1931.
- Barucci, M. A., M. Lazzarin, T. Owen, C. Barbieri, and M. Fulchignoni 1994. Near-infrared spectroscopy of dark asteroids. *Icarus* **110**, 287–291.
- Bell, J. F. III, J. B. Pollack, T. R. Geballe, D. P. Cruikshank, and R. Freedman 1994. Spectroscopy of Mars from 2.04 to 2.44 μm during the 1993 opposition: Absolute calibration and atmospheric vs mineralogic origin of narrow absorption features. *Icarus* **111**, 106–123.
- Bernatowicz, T. J. 1997. Presolar grains from meteorites. In *From Stardust to Planetesimals* (Y. J. Pendleton and A. G. G. M. Tielens, Eds.), Astron. Soc. Pacific Conf. Series, pp. 227–251. Astronomical Society of the Pacific, San Francisco, CA.
- Bernstein, M. P., S. A. Sandford, L. J. Allamandola, and S. Chang 1994. Infrared spectrum of matrix-isolated hexamethylenetetramine in Ar and H₂O at cryogenic temperatures. *J. Phys. Chem.* **98**, 12206–12210.
- Bernstein, M. P., S. A. Sandford, L. J. Allamandola, S. Chang, and M. A. Scharberg 1995. Organic compounds produced by photolysis of realistic interstellar and cometary ice analogs containing methanol. *Astrophys. J.* **454**, 327–344.
- Binzel, R. 1992. The optical spectrum of 5145 Pholus. *Icarus* **99**, 238–240.
- Bockelée-Morvan, D., P. Colom, J. Crovisier, D. Despois, and G. Paubert 1991. Microwave detection of hydrogen sulphide and methanol in Comet Austin (1989c1). *Nature* **350**, 318–320.
- Bradley, J. P., D. E. Brownlee, and T. P. Snow 1997. GEMS and other pre-accretionally irradiated grains in interplanetary dust particles. In *From Stardust to Planetesimals* (Y. J. Pendleton and A. G. G. M.

- Tielens, Eds.), *Astron. Soc. Pacific Conf. Series*, pp. 217–225. Astronomical Society of the Pacific, San Francisco, CA.
- Brown, R. H., D. P. Cruikshank, Y. J. Pendleton, and G. J. Veeder 1997. Surface composition of Kuiper Belt object 1993 SC. *Science* **276**, 937–939.
- Brown, R. H., D. P. Cruikshank, Y. J. Pendleton, and G. J. Veeder 1998. Detection of water ice on Centaur object 1997 CU26. *Science* **280**, 1430–1432.
- Buie, M. J., and S. J. Bus 1992. Physical observations of (5145) Pholus. *Icarus* **100**, 288–294.
- Campins, H., G. H. Rieke, and M. J. Lebofsky 1985. Absolute calibration of photometry at 1 through 5 μm . *Astron. J.* **90**, 896–899.
- Chiar, J. E., Y. J. Pendleton, T. R. Geballe, and A. G. G. M. Tielens 1998. Near-infrared spectroscopy of the protoplanetary nebula CRL 618 and the origin of the hydrocarbon dust component in the interstellar medium. *Astrophys. J.* **507**, in press.
- Clark, R. N., G. A. Swayze, A. J. Gallagher, T. V. V. King, and W. M. Calvin 1993. The U.S.G.S. Digital Spectral Library: Version 1: 0.2 to 3.0 μm . U.S. Geological Survey Open File Report 93-592.
- Cloutis, E. A. 1989. Spectral reflectance properties of hydrocarbons: Remote sensing implications. *Science* **245**, 165–168.
- Cloutis, E. A., M. J. Gaffey, and T. F. Moslow 1994. Spectral reflectance properties of carbon-bearing materials. *Icarus* **107**, 276–287.
- Cronin, J. R., S. Pizzarello, and D. P. Cruikshank 1988. Organic matter in carbonaceous chondrites, planetary satellites, asteroids, and comets. In *Meteorites and the Early Solar System* (J. F. Kerridge and M. S. Matthews, Eds.), pp. 819–857. Univ. of Arizona Press, Tucson.
- Crovisier, J., K. Leech, D. Bockelée-Morvan, T. Y. Brooke, M. S. Hanner, B. Altieri, H. U. Keller, and E. Lellouch 1997. The spectrum of Comet Hale–Bopp (C/1995 O1) observed with the Infrared Space Observatory at 2.9 astronomical units from the Sun. *Science* **275**, 1904–1907.
- Cruikshank, D. P. 1987. Dark matter in the Solar System. *Adv. Space Res.* **7**(5), 109–120.
- Cruikshank, D. P. 1989. Dark surfaces of asteroids and comets: Evidence for macromolecular carbon compounds. *Adv. Space Res.* **9**(2), 65–71.
- Cruikshank, D. P. 1997. Organic matter in the outer Solar System: From the meteorites to the Kuiper Belt. In *From Stardust to Planetesimals* (Y. J. Pendleton and A. G. G. M. Tielens, Eds.), *Astron. Soc. Pacific Conf. Series*, pp. 315–333. Astronomical Society of the Pacific, San Francisco, CA.
- Cruikshank, D. P., and J. F. Kerridge 1992. Organic material in asteroids, meteorites, and planetary satellites. In *Exobiology in Solar System Exploration* (G. Carle, D. Schwartz, and J. Huntington, Eds.), NASA SP-512, pp. 159–175.
- Cruikshank, D. P., L. J. Allamandola, W. K. Hartmann, D. J. Tholen, R. H. Brown, C. N. Matthews, and J. F. Bell 1991. Solid CN bearing material on outer Solar System bodies. *Icarus* **94**, 345–353.
- Cruikshank, D. P., L. V. Moroz, T. R. Geballe, C. M. Pieters, and J. F. Bell, III 1993. Asphaltite-like organics on planetesimal 5145 Pholus. *Bull. A. A. S.* **25**, 1125–1126. [Abstract]
- Cruikshank, D. P., T. L. Roush, J. M. Moore, M. V. Sykes, T. C. Owen, M. J. Bartholomew, R. H. Brown, and K. A. Tryka 1997. The surfaces of Pluto and Charon. In *Pluto and Charon* (S. A. Stern and D. J. Tholen, Eds.), pp. 221–267. Univ. of Arizona Press, Tucson.
- Cruikshank, D. P., T. L. Roush, T. C. Owen, E. Quirico, and C. deBergh 1998. The surface compositions of Triton, Pluto, and Charon. In *Solar System Ices* (B. Schmitt, C. deBergh, and M. Festou, Eds.), pp. 655–684. Kluwer, Dordrecht.
- Davies, J. K., and M. V. Sykes 1992. 5145–1992 AD. *IAU Circ.* 5480 (20 March).
- Davies, J. K., T. Geballe, D. Cruikshank, T. Owen, and C. deBergh 1995. Comet C/1995 O1. *IAU Circ.* 6225 (11 September).
- Davies, J. K., N. McBride, S. L. Ellison, S. F. Green, and D. R. Ballantyne 1998. Optical and infrared photometry of six Centaurs. *Icarus* **134**, 213–227.
- Davies, J. K., T. L. Roush, D. P. Cruikshank, M. J. Bartholomew, T. R. Geballe, T. C. Owen, and C. de Bergh 1997. The detection of water ice in Comet Hale–Bopp. *Icarus* **127**, 238–245.
- Davies, J. K., J. Spencer, M. Sykes, D. Tholen, and S. Green 1993a. 5145 Pholus. *IAU Circ.* 5698 (27 January).
- Davies, J. K., M. V. Sykes, and D. P. Cruikshank 1993b. Near-infrared photometry and spectroscopy of the unusual minor planet 5145 Pholus (1992AD). *Icarus* **102**, 166–169.
- Davies, J. K., D. J. Tholen, and D. R. Ballantyne 1996. Infrared observations of distant asteroids. In *Completing the Inventory of the Solar System* (T. W. Rettig and J. M. Hahn, Eds.), *Astron. Soc. Pacific Conf. Series*, pp. 97–105. Astronomical Society of the Pacific, San Francisco, CA.
- Ehrenfreund, P., J. J. Boon, J. Comandeur, C. Sagan, W. R. Thompson, B. N. Khare, and G. Israel 1995. Analytical pyrolysis experiments of Titan aerosol analogues in preparation for the Cassini–Huygens mission. *Adv. Space Res.* **15**(3), 335.
- Falk, M., and E. Whalley 1961. Infrared spectra of methanol and deuterated methanols in gas, liquid, and solid phases. *J. Chem. Phys.* **34**, 1554–1568.
- Fink, U., M. Hoffmann, W. Grundy, M. Hicks, and W. Sears 1992. The steep red spectrum of 1992 AD: An asteroid covered with organic material? *Icarus* **97**, 145–149.
- Fomenkova, M. N. 1997. Organic components of cometary dust. In *From Stardust to Planetesimals* (Y. J. Pendleton and A. G. G. M. Tielens, Eds.), *Astron. Soc. Pacific Conf. Series*, pp. 415–421. Astronomical Society of the Pacific, San Francisco, CA.
- Geballe, T. R., J. Chiar, Y. J. Pendleton, and A. G. G. M. Tielens 1998. The 3.4 microns absorption feature in CRL 618. In *ISO's View on Stellar Evolution*, in press.
- Greenberg, J. M. 1982. What are comets made of? A model based on interstellar dust. In *Comets* (L. L. Wilkening, Ed.), pp. 131–163. Univ. of Arizona Press, Tucson.
- Greenberg, J. M. 1996. Comets as samplers of interstellar dust. In *The Cosmic Dust Connection* (J. M. Greenberg, Ed.), pp. 443–458. Kluwer, Dordrecht.
- Greenberg, J. M. 1998. Making a comet nucleus. *Astron. Astrophys.* **330**, 375–380.
- Grim, R. J. A., F. Baas, J. M. Greenberg, T. R. Geballe, and W. Schutte 1991. Detection of solid methanol toward W33A. *Astron. Astrophys.* **243**, 473–477.
- Hanel, R., B. Conrath, F. M. Flasar, V. Kunde, W. Maguire, J. Pearl, J. Pirraglia, R. Samuelson, L. Herath, M. Allison, D. Cruikshank, D. Gautier, P. Gierasch, L. Horn, R. Koppány, and C. Ponnameruma 1981. Infrared observations of the saturnian system from Voyager 1. *Science* **212**, 192–200.
- Hapke, B. 1993. *Theory of Reflectance and Emittance Spectroscopy*. Cambridge Univ. Press, Cambridge.
- Hartmann, W. K., D. J. Tholen, and D. P. Cruikshank 1986. The relationship of active comets, “extinct” comets, and dark asteroids. *Icarus* **69**, 33–50.
- Hartmann, W. K., D. J. Tholen, K. J. Meech, and D. P. Cruikshank 1990. 2060 Chiron: Colorimetry and possible cometary behavior. *Icarus* **83**, 1–15.
- Hiroi, T., and H. Takeda 1990. A method to determine silicate abundances from reflectance spectra with applications to asteroid 29 Amphitrite associating it with primitive achondrite meteorites. *Icarus* **88**, 205–227.

- Hoban, S., M. J. Mumma, D. C. Reuter, M. DiSanti, R. R. Joyce, and A. Storrs 1991. A tentative identification of methanol as the progenitor of the 3.52 μm feature in several comets. *Icarus* **93**, 122–134.
- Hoffmann, M., U. Fink, W. M. Grundy, and M. Hicks 1993. Photometric and spectroscopic observations of 5145 Pholus. *J. Geophys. Res.* **98**, 7403–7407.
- Howell, E. S. 1995. *Probing Asteroid Composition Using Visible and Near-Infrared Spectroscopy*. Ph.D. thesis, Univ. of Arizona, Tucson.
- Howell, E. S., R. Marcialis, R. Cutri, M. Nolan, L. Lebofsky, and M. Sykes 1992. 1992AD, *IAU Circ.* 5449 (12 February).
- Huebner, W. F. 1987. First polymer in space identified in Comet Halley. *Science* **237**, 628–630.
- Jenniskens, P., and D. F. Blake 1996. Crystallization of amorphous water ice in the Solar System. *Astrophys. J.* **473**, 1104–1113.
- Jewitt, D. C., B. T. Soifer, G. Neugebauer, K. Matthews, and G. E. Danielson 1982. Visual and infrared observations of the distant Comets P/Stephan–Oterman (1980g), Panther (1980u), and Bowell (1980b). *Astron. J.* **87**, 1854–1866.
- Jewitt, D. C., and J. X. Luu 1995. The Solar System beyond Neptune. *Astrophys. J.* **109**, 1867–1876.
- Jewitt, D. C., and J. X. Luu 1998. Optical-infrared spectral diversity in the Kuiper Belt. *Astron. J.*, in press.
- Jewitt, D. C., and K. J. Meech 1988. The absence of a color–distance trend in comets. *Astron. J.* **96**, 1723–1730.
- Khare, B. N., C. Sagan, E. T. Arakawa, F. Suits, T. A. Callcott, and M. W. Williams 1984a. Optical constants of organic tholin produced in a simulated Titanian atmosphere: From soft X-ray to microwave frequencies. *Icarus* **60**, 127–137.
- Khare, B. N., C. Sagan, W. R. Thompson, E. T. Arakawa, F. Suits, T. A. Callcott, M. W. Williams, S. Shrader, H. Ogino, T. O. Willingham, and B. Nagy 1984b. The organic aerosols of Titan. *Adv. Space Res.* **4**, 59–68.
- Khare, B. N., C. Sagan, H. Ogino, B. Nagy, C. Er, K. H. Schram, and E. T. Arakawa 1986. Amino acids derived from Titan tholins. *Icarus* **68**, 176–184.
- Khare, B. N., W. R. Thompson, B., G. J. P. T. Murray, C. F. Chyba, C. Sagan, and E. T. Arakawa 1989. Solid organic residues produced by irradiation of hydrocarbon-containing H_2O and $\text{H}_2\text{O}/\text{NH}_3$ ices: Infrared spectroscopy and astronomical implications. *Icarus* **79**, 350–361.
- Khare, B. N., W. R. Thompson, L. Cheng, C. Chyba, C. Sagan, E. T. Arakawa, C. Meisse, and P. S. Tuminello 1993. Production and optical constants of ice tholin from charged particle irradiation of (1:6) $\text{C}_2\text{H}_6/\text{H}_2\text{O}$ at 77 K. *Icarus* **103**, 290–300.
- Kissel, J., and F. R. Krueger 1987. The organic component in dust from Comet Halley as measured by the PUMA mass spectrometer on board Vega 1. *Nature* **326**, 755–760.
- Lacy, J. H., F. Baas, L. J. Allamandola, S. E. Persson, P. J. McGregor, C. J. Lonsdale, T. R. Geballe, and C. E. P. van de Bult 1984. 4.6 micron absorption features due to solid phase CO and cyano group molecules toward compact infrared sources. *Astrophys. J.* **276**, 533–543.
- Levison, H. F., and M. J. Duncan 1993. The gravitational sculpting of the Kuiper belt. *Astrophys. J. Lett.* **406**, L35–L38.
- Lucey, P. G. 1998. Model near-infrared optical constants of olivine and pyroxene as a function of iron content. *J. Geophys. Res.* **103**, 1703–1713.
- Luu, J. X. 1993. Spectral diversity among the nuclei of comets. *Icarus* **104**, 138–148.
- Luu, J., D. Jewitt, and E. Cloutis 1994. Near-infrared spectroscopy of primitive Solar System objects. *Icarus* **109**, 133–144.
- Marsden, B. G. 1992. *IAU Circ.* 5480 (20 March).
- McCord, T. B., R. W. Carlson, W. D. Smythe, G. B. Hansen, R. N. Clark, C. A. Hibbitts, F. P. Fanale, J. C. Granahan, M. Segura, D. L. Matson, T. V. Johnson, and P. D. Martin 1997. Organics and other molecules in the surfaces of Callisto and Ganymede. *Science* **278**, 271–275.
- McDonald, G. D., W. R. Thompson, M. Heinrich, B. N. Khare, and C. Sagan 1994. Chemical investigation of Titan and Triton tholins. *Icarus* **108**, 137–145.
- Meech, K. J., and M. J. S. Belton 1990. The atmosphere of 2060 Chiron. *Astron. J.* **100**, 1132–1138.
- Mitchell, D. L., R. P. Lin, K. A. Anderson, C. W. Carlson, D. W. Curtis, A. Korth, H. Rème, J. A. Sauvard, C d’Uston, and D. A. Mendis. 1987. Evidence for chain molecules enriched in carbon, hydrogen, and oxygen in Comet Halley. *Science* **237**, 626–628.
- Mitchell, D. L., R. P. Lin, C. W. Carlson, A. Korth, H. Rème, and D. A. Mendis 1992. The origin of complex organic ions in the coma of Comet Halley. *Icarus* **98**, 125–133.
- Moroz, L. V., C. M. Pieters, and M. V. Akhmanova 1991. Spectroscopy of solid carbonaceous materials: Implications for dark surfaces of outer belt asteroids. *Lunar Planet. Sci. Conf.* 22nd, 925–926.
- Moroz, L. V., C. M. Pieters, and M. V. Akhmanova 1992. Why the surfaces of outer belt asteroids are dark and red. *Lunar Planet. Sci. Conf.* 23rd, 931–932.
- Mueller, B. E. A., D. J. Tholen, W. K. Hartmann, and D. P. Cruikshank 1992. Extraordinary colors of asteroidal object (5145) 1992 AD. *Icarus* **97**, 150–154.
- Mumma, M. J., P. R. Weissman, and S. A. Stern 1993. Comets and the origin of the Solar System: Reading the Rosetta Stone. In *Protostars and Planets III* (E. H. Levy and J. I. Lunine, Eds.), pp. 1177–1252. Univ. of Arizona Press, Tucson.
- Ockman, N. 1957. *The Infrared-Spectra and Raman-Spectra of Single Crystals of Ordinary Ice*. Dissertation, Univ. Michigan, Ann Arbor, MI.
- Owen, T. C., D. P. Cruikshank, C. de Bergh, and T. R. Geballe 1995. Dark matter in the outer Solar System. *Adv. Space Res.* **16**(2), 41–49.
- Palumbo, M. E., G. Strazzulla, Y. J. Pendleton, and A. G. G. M. Tielens 1998. *Astrophys. J.*, submitted for publication.
- Papoular, R., J. Breton, G. Gensterblum, I. Nenner, R. J. Papoular, and J.-J. Pireaux 1993a. The vis/UV spectrum of coals and the interstellar extinction curve. *Astron. Astrophys.* **270**, L5–L8.
- Papoular, R., J. Conard, M. Giuliano, J. Kister, and G. Mille 1989. A coal model for the carriers of the unidentified IR bands. *Astron. Astrophys.* **217**, 204–208.
- Papoular, R., K. Ellis, O. Guillois, C. Reynaud, and I. Nenner 1993b. New developments of the coal model of interstellar dust. *J. Chem. Soc. Faraday Trans.* **89**, 2289–2295.
- Pendleton, Y. J., S. A. Sandford, L. J. Allamandola, A. G. G. M. Tielens, and K. Sellgren 1994. Near-infrared absorption spectroscopy of interstellar hydrocarbon grains. *Astrophys. J.* **437**, 683–696.
- Pendleton, Y. J., A. G. G. M. Tielens, A. T. Tokunaga, and M. P. Bernstein 1998. The interstellar 4.62 μm band. *Astrophys. J.*, in press.
- Pollack, J. B., D. Hollenbach, S. Beckwith, D. P. Simonelli, T. Roush, and W. Fong 1994. Composition and radiative properties of grains in molecular clouds and accretion disks. *Astrophys. J.* **421**, 615–639.
- Roush, T. L. 1994. Charon: More than water ice? *Icarus* **108**, 243–254.
- Roush, T. 1996. Near-IR (0.8–2.5 μm) optical constants of water ice at 100K. *Lunar Planet. Sci. Conf.* 27th, 1107–1108.
- Roush, T. L., J. B. Pollack, F. C. Witteborn, J. D. Bregman, and J. P. Simpson 1990. Ice and minerals on Callisto: A reassessment of the reflectance spectra. *Icarus* **86**, 355–382.
- Sagan, C., and B. N. Khare 1979. Tholins: Organic chemistry of interstellar grains and gas. *Nature* **227**, 102–107.

- Sagan, C., B. N. Khare, and J. S. Lewis 1984. Organic matter in the Saturn system. In *Saturn* (T. Gehrels and M. S. Matthews, Eds.), pp. 788–807. Univ. of Arizona Press, Tucson.
- Sandford, S. A., and L. J. Allamandola 1993. Condensation and vaporization studies of CH₃OH and NH₃ ices: Major implications for astrochemistry. *Astrophys. J.* **417**, 815–825.
- Sandford, S. A., L. J. Allamandola, A. G. G. M. Tielens, K. Sellgren, M. Tapia, and Y. Pendleton 1991. The interstellar C-H stretching band near 3.4 microns: Constraints on the composition of organic material in the diffuse interstellar medium. *Astrophys. J.* **371**, 607–620.
- Schulze, H., J. Kissel, and E. K. Jessberger 1997. Chemistry and mineralogy of Comet Halley's dust. In *From Stardust to Planetesimals* (Y. J. Pendleton and A. G. G. M. Tielens, Eds.), Astron. Soc. Pacific Conf. Series, pp. 397–414. Astronomical Society of the Pacific, San Francisco, CA.
- Schutte, W. A. 1988. *The Evolution of Interstellar Organic Grain Mantles*. Ph.D. thesis, Univ. of Leiden, The Netherlands.
- Scotti, J. V. 1992 AD. *IAU Circ. 5434*, 23 January.
- Skinner, C. J., A. G. G. M. Tielens, M. J. Barlow, and K. Justtanont 1992. Methanol ice in the protostar GL 2136. *Astrophys. J.* **399**, L79–L82.
- Strazzulla, G., and R. E. Johnson 1991. Irradiation effects on comets and cometary debris. In *Comets in the Post-Halley Era* (R. L. Newburn, Jr., M. Neugebauer, and J. Rahe, Eds.), Vol. 1, pp. 243–275. Kluwer, Dordrecht.
- Strazzulla, G., A. C. Castorina, and M. E. Palumbo 1995. Ion irradiation of astrophysical ices. *Planet. Space Sci.* **43**, 1247–1251.
- Tegler, S. C., and W. Romanishin 1998. Two distinct populations of Kuiper belt objects. *Nature* **392**, 49–51.
- Tegler, S. C., D. A. Weintraub, L. J. Allamandola, S. A. Sandford, T. W. Rettig, and H. Campins 1993. Detection of the 2165 inverse centimeter (4.619 micron) XCN band in the spectrum of L1551 IRS 5. *Astrophys. J.* **411**, 260–265.
- Tegler, S. C., D. A. Weintraub, T. W. Rettig, Y. J. Pendleton, D. C. B. Whittet, and C. A. Kulesa 1995. Evidence for chemical processing of precometary ice grains in circumstellar environments of pre-main-sequence stars. *Astrophys. J.* **439**, 279–287.
- Thompson, W. R., T. J. Henry, J. M. Schwartz, B. N. Khare, and C. Sagan 1991. Plasma discharge in N₂+CH₄ at low pressures: Experimental results and applications to Titan. *Icarus* **90**, 57–73.
- Thompson, W. R., B. G. J. P. T. Murray, B. N. Khare, and C. Sagan 1987. Coloration and darkening of methane clathrate and other ices by charged particle irradiation: Applications to the outer Solar System. *J. Geophys. Res.* **92**, 14,933–14,947.
- Tielens, A. G. G. M., and L. J. Allamandola 1987. Evolution of interstellar dust. In *Physical Processes in Interstellar Clouds* (G. E. Morfill and M. Scholer, Eds.), pp. 333–376. Reidel, Dordrecht.
- Tielens, A. G. G. M., and D. C. B. Whittet 1997. Ices in star forming regions. In *Molecules in Astrophysics: Probes and Processes* (E. F. van Dishoeck, Ed.), pp. 45–60. Kluwer, Dordrecht.
- Warren, S. G. 1984. Optical constants of ice from the ultraviolet to the microwave. *Appl. Opt.* **23**, 1206–1225.
- Waters, L. B. F. M., C. Waelkens, H. van Winckel, F. J. Molster, A. G. G. M. Tielens, J. Th. van Loon, P. W. Morris, J. Cami, J. Bouwman, A. de Koter, T. de Jong, and Th. de Graauw 1998. An oxygen-rich dust disk surrounding an evolved star in the Red Rectangle. *Nature* **391**, 868–871.
- Whittet, D. C. B., and A. G. G. M. Tielens 1997. Infrared observations of interstellar dust absorption features. In *From Stardust to Planetesimals* (Y. J. Pendleton and A. G. G. M. Tielens, Eds.), pp. 161–178. Astron. Soc. Pacific Conf. Series. Astronomical Society of the Pacific, San Francisco, CA.
- Wilson, P. D. 1997. *Models of Organic-Rich Surfaces in the Outer Solar System*. Ph.D. thesis, Cornell Univ., Ithaca, NY.
- Wilson, P. D., C. Sagan, and W. R. Thompson 1994. The organic surface of 5145 Pholus: Constraints set by scattering theory. *Icarus* **107**, 288–303.